A comprehensive sulfur and oxygen isotope study of sulfur cycling in a shallow, hyper-euxinic meromictic lake

William P. Gilhooly III[a,b,*], Christopher T. Reinhard[a,c], Timothy W. Lyons[a]

[a]Department of Earth Sciences, University of California, 900 University Avenue, Riverside, CA 92521, USA
[b]Department of Earth Sciences, Indiana University-Purdue University Indianapolis, SL118, 723 W. Michigan Street, Indianapolis, IN 46202, USA
[c]School of Earth & Atmospheric Sciences, Georgia Institute of Technology, 311 Ferst Drive, Atlanta, GA 30332, USA

*Corresponding author. Current address: Department of Earth Sciences, Indiana University-Purdue University Indianapolis, SL118, 723 W. Michigan Street, Indianapolis, IN 46202, USA. E-mail address: wgilhool@iupui.edu (W. Gilhooly).

This is the author's manuscript of the article published in final edited form as:

Gilhooly III, W. P., Reinhard, C. T., & Lyons, T. W. (n.d.). A comprehensive sulfur and oxygen isotope study of sulfur cycling in a shallow, hyper-euxinic meromictic lake. Geochimica et Cosmochimica Acta. http://doi.org/10.1016/j.gca.2016.05.044

Abstract

Mahoney Lake is a permanently anoxic and sulfidic (euxinic) lake that has a dense plate of purple sulfur bacteria positioned at mid-water depth (~ 7 m) where free sulfide intercepts the photic zone. We analyzed the isotopic composition of sulfate ($\delta^{34}S_{SO4}$ and $\delta^{18}O_{SO4}$), sulfide ($\delta^{34}S_{H2S}$), and the water ($\delta^{18}O_{H2O}$) to track the potentially coupled processes of dissimilatory sulfate reduction and phototrophic sulfide oxidation within an aquatic environment with extremely high sulfide concentrations (>30 mM). Large isotopic offsets observed between sulfate and sulfide within the monimolimnion ($\delta^{34}S_{SO4\text{-}H2S}$ = 51‰) and within pore waters along the oxic margin ($\delta^{34}S_{SO4\text{-}H2S}$ >50‰) are consistent with sulfate reduction in both the sediments and the anoxic water column. Given the high sulfide concentrations of the lake, sulfur disproportionation is likely inoperable or limited to a very narrow zone in the chemocline, and therefore the large instantaneous fractionations are best explained by the microbial process of sulfate reduction. Pyrite extracted from the sediments reflects the isotopic composition of water column sulfide, suggesting that pyrite buried in the euxinic depocenter of the lake formed in the water column. The offset between sulfate and dissolved sulfide decreases at the chemocline ($\delta^{34}S_{SO4\text{-}H2S}$ = 37‰), a trend possibly explained by elevated sulfate reduction rates and inconsistent with appreciable disproportionation within this interval. Water column sulfate exhibits a linear response in $\delta^{18}O_{SO4}$-$\delta^{34}S_{SO4}$ and the slope of this relationship suggests relatively high sulfate reduction rates that appear to respond to seasonal changes in the productivity of purple sulfur bacteria. Although photosynthetic activity within the microbial plate influences the $\delta^{18}O_{SO4}$-$\delta^{34}S$ relationship, the biosignature for photosynthetic sulfur bacteria is restricted to the oxic/anoxic transition zone and is apparently minor relative to the more prevalent process of sulfate reduction operative throughout the light-deprived deeper anoxic water column and sediment pore waters.

1. Introduction

Sulfur isotope compilations of sedimentary pyrite and sulfates (gypsum, barite, carbonate-associated sulfate) have provided proxy evidence for the increase in atmospheric oxygen from the Archean to the present. Three distinct stages have been recognized in the sulfur isotope record based on mass conservative ($^{34}S/^{32}S$) and mass-independent ($^{33}S/^{32}S$) fractionation effects. Small $\delta^{34}S$ fractionations (Canfield, 1998), associated with low oceanic sulfate levels (< 2.5 μM) in the Archean (Habicht et al., 2002; Crowe et al., 2014), are congruent with $\Delta^{33}S$ photochemical isotope effects preserved under low atmospheric oxygen levels (Farquhar et al., 2000). This stage ends with the Great Oxidation Event marked by an increase in $\delta^{34}S$ fractionations coincident with the loss of mass-independent signatures ~2.3-2.4 billion years ago (Bekker et al., 2004), indicating that oxygen accumulated to significant concentrations in the atmosphere. The third state, characterized by frequently large fractionations perhaps linked to a strongly oxidative sulfur cycling and analogous to isotopic patterns seen today ($\Delta^{34}S_{sulfate\text{-}sulfide} > 50‰$), commenced during the Neoproterozoic (1050 to 640 million years ago) (Canfield & Teske, 1996; Canfield, 2001).

The isotopic offset ($\Delta^{34}S_{sulfate\text{-}sulfide} = \delta^{34}S_{sulfate} - \delta^{34}S_{sulfide}$) imparted during dissimilatory sulfate reduction can be large in magnitude, with $\Delta^{34}S_{sulfate\text{-}sulfide}$ exceeding 60‰ (Canfield et al., 2010; Sim et al., 2011), or muted (~ 0‰) at low sulfate concentrations (Harrison & Thode, 1958; Habicht et al., 2002). Similar offsets are produced by the oxidative sulfur cycle, ranging from the potentially large isotope effects (~20‰) that can occur during sulfur disproportionation (Canfield & Thamdrup, 1994; Habicht et al., 1998; Böttcher et al., 2001) to small isotope effects (± 5‰) produced during chemolithotrophic sulfide oxidation (Fry et al., 1986) and anoxygenic

70 photosynthesis (Fry et al., 1984; Fry, 1986; Zerkle et al., 2009; Brabec et al., 2012). An
71 otherwise robust biosignature for sulfate reduction in modern sediments thus becomes non-
72 diagnostic under sulfate-limited conditions as postulated for the Archean ocean or periods of
73 rapid expansion of the oceanic sulfate pool such as the Neoproterozoic, when many reactions
74 within the biologically mediated sulfur cycle may be operative. For example, the various
75 explanations for an increase in the magnitude of sulfur isotope fractionations during the
76 Neoproterozoic include an increased prominence of nonphotosynthetic oxidative sulfur
77 metabolisms and associated disproportionation of the resulting intermediate sulfur species
78 (Canfield & Teske, 1996; Johnston et al., 2005; Fike et al., 2006), reoxidation effects mediated
79 by the onset of bioturbation (Canfield & Farquhar, 2009), and possibly reservoir effects linked
80 with rising and falling sulfate concentrations within an evolving oceanic sulfur pool (Hurtgen et
81 al., 2005).
82
83 The isotopic composition of oxygen bound in sulfate ($\delta^{18}O_{SO4}$) may provide an additional vector
84 to better interpret the microbial processes responsible for sulfate synthesis and cycling over
85 geologic timescales. Provided the associated isotope effects are constrained, $\delta^{18}O_{SO4}$ can be a
86 powerful tool for tracing the ultimate source of sulfate to the ocean, given that the oxygen
87 incorporated into the sulfate during sulfide oxidation can derive from either ambient water (H_2O)
88 or the atmosphere (O_2). On a global basis, gypsum dissolution and oxidative pyrite weathering
89 (the inputs) balance the outputs via evaporite precipitation and sulfate reduction with
90 concomitant pyrite burial (Holser et al., 1979; Claypool et al., 1980). Tracking the sulfate-
91 oxygen budget through these isotopically distinct reservoirs is complicated by oxygen isotope
92 exchange at low pH (Hoering & Kennedy, 1957; Lloyd, 1968; Chiba & Sakai, 1985), post-

93 diagenetic alteration (Turchyn et al., 2009), and numerous other processes that overprint the
94 oxygen isotope composition of sulfate (Bottrell & Newton, 2006; Turchyn & Schrag, 2006).
95
96 Sulfur isotopes are relatively insensitive to inorganic sulfide oxidation effects, but sulfate formed
97 from sulfide oxidation will carry different proportions of oxygen derived from water ($\delta^{18}O \leq$
98 0‰) and/or atmospheric oxygen ($\delta^{18}O = 23.5$‰) depending on the oxidation pathway (Taylor &
99 Wheeler, 1984; van Everdingen & Krouse, 1985; Balci et al., 2007; Calmels et al., 2007; Balci et
100 al., 2012). The oxidation of sulfide coupled to iron reduction derives oxygen entirely from water
101 and results in $\delta^{18}O_{SO4}$ values lower than those produced by oxidation with molecular oxygen
102 (Calmels et al., 2007). Hydrothermal sulfur inputs (~ 0‰) may be difficult to differentiate from
103 biological cycling within a low sulfate reservoir; however, $\delta^{18}O_{SO4}$ produced by photosynthetic
104 bacteria may reflect the isotopic composition of the parent water (Brabec et al., 2012).
105
106 Environmental conditions in the Paleo- and Mesoproterozoic, when atmospheric oxygen
107 concentrations were still relatively low, and large portions of the oceans were anoxic and sulfidic
108 (euxinic), were conducive to widespread carbon fixation by anoxygenic photosynthesis
109 (Johnston et al., 2009). Phototrophic sulfur bacteria oxidize sulfide and fix carbon dioxide in the
110 presence of sunlight without producing oxygen. Sulfide is oxidized to intracellular elemental
111 sulfur, and the internal sulfur stores are ultimately oxidized to sulfate when sulfide becomes
112 limiting (< 1 mM) (Overmann & Pfennig, 1992). In the geologic record, this ecological niche is
113 termed "photic zone euxinia," and organic biomarkers of sulfide-oxidizing phototrophs can
114 provide proxy evidence for free sulfide at shallow depths in the water column (Brocks et al.,
115 2005; Brocks & Schaeffer, 2008) provided the organisms were pelagic (Meyer et al., 2011).

116 Biological oxidation of sulfide by anoxygenic photosynthesis may have contributed to the
117 formation of sulfate in the Proterozoic water column (Johnston et al., 2009). With limited
118 organic biomarker and geochemical evidence for widespread primary production by anoxygenic
119 sulfur bacteria (Lyons et al., 2004), and the potential for metabolic overlap with cyanobacteria
120 capable of sulfide oxidation but without a distinctive biomarker signature for this process
121 (Johnston et al., 2009), additional proxies are needed to fingerprint the paleoecological and
122 biogeochemical signals associated with euxinia in the photic zone. Paired $\delta^{34}S$ and $\delta^{18}O$ data
123 from ancient sulfates (gypsum, barite, or carbonate-associated-sulfate) may offer an additional
124 constraint on the history and ecological distribution of photosynthetic S-oxidation. Sulfate-
125 oxygen can fractionate during sulfate reduction, but the extent of isotopic enrichment is
126 controlled either by kinetic isotope effects imparted during intracellular enzymatic steps or
127 equilibrium oxygen exchange with ambient water (Brunner et al., 2005; Brunner et al., 2012;
128 Antler et al., 2013). An improved understanding of these processes can be gained from modern
129 natural environments.
130
131 The primary objective of this study was to track microbial sulfur oxidation and reduction in
132 density stratified Mahoney Lake as a modern analog for biotic pathways that may have generated
133 oxidants in Earth's early ocean. Free dissolved sulfide ($[H_2S]$ = 30 mM) in the photic zone of the
134 water column supports a perennial plate of purple sulfur bacteria (Northcote & Halsey, 1969;
135 Northcote & Hall, 1983; Overmann et al., 1991; Overmann et al., 1996). The purple sulfur
136 bacterium is a member of *Chromatiaceae* and is designated as strain ML1 (Hamilton et al.,
137 2014). Although found at mid-water depth of the lake, ML1 is most closely related to a marine
138 benthic purple sulfur bacteria *Thiohalocapsa* (Hamilton et al., 2014). Such observations have

significance when relating biomarker distribution to microbial ecology and inferred environmental conditions (Meyer et al., 2011). The euxinic conditions are broadly consistent with chemical properties for many Proterozoic ocean models (Reinhard et al., 2013). However, the lake also has high sulfate concentrations ($[SO_4]$ > 300 mM) that are inconsistent with early analogs and indeed are more than ten times the concentration in the modern ocean. At the same time, the large reservoir helps maximize the isotopic offset for sulfate reduction ($\Delta^{34}S_{sulfate\text{-}sulfide}$ >50‰). In other words, the isotopic offsets are controlled by biological processing rather than by the size of the sulfate pool. The biosignature for dissimilatory sulfate reduction in Mahoney Lake is thus distinct from the small offsets produced under sulfate-limited conditions that would otherwise overlap with sulfur isotope fractionations produced by sulfide oxidizing phototrophic bacteria. As such, Mahoney Lake provides a novel natural laboratory for studying sulfur cycling. We present paired sulfur and oxygen isotope compositions of dissolved sulfate ($\delta^{34}S_{SO4}$ and $\delta^{18}O_{SO4}$) relative to the sulfur isotope properties of product sulfides (either dissolved or sedimentary) to explore isotope effects associated with sulfate reduction and anaerobic sulfide oxidation (and thus biologically mediated sulfate generation) by anoxygenic photosynthetic bacteria.

2. Materials and Methods

Site description

Mahoney Lake (49°17'N; 119°35'W; elevation 47.15 m) is a permanently stratified (meromictic) lake in the Okanagan Valley, British Columbia (Figure 1). Within the same catchment, Green Lake (49°18'N, 119°34'W, 490.7 m) fully mixes during fall and spring overturn (dimictic). Both are shallow (~15 m), saline, terminal lakes. The Okanagan Valley is an arid region within the

southern interior of a province that receives an average of 265 mm of total annual precipitation (rain and snow). Mean monthly temperatures range from -14.3ºC to 23.5ºC (www.climate.weatheroffice.gc.ca; station 1126150; precipitation and temperature records 1941 to 2010).

The lake drainage area is located within an extensional basin known as the White Lake Basin (Figure 1). The regional geology is dominated by a complex series of normal faults, fractured bedding planes, and jointed volcanic formations that promote groundwater circulation (Lewis, 1984; Michel et al., 2002). Both lakes straddle a north-south trending fault line that bisects the drainage basin (Northcote & Hall, 1983). The bedrock geology to the east of the fault is comprised of cherts, greenstones, schists, and granitic intrusions (Northcote & Hall, 1983; Church, 2002) (Figure 1). The western extent of the catchment contains ultramafic volcanic rocks and lavas (Northcote & Hall, 1983; Church, 2002). Salts (Na-Ca-Mg-SO_4) derived from the weathering of metavolcanic rocks from the Marron Formation (Eocene) in the surrounding watershed contribute to the high conductivity and total dissolved solid load of Mahoney Lake (Northcote & Hall, 1983).

Mahoney Lake (136.2×10^4 m^3, 19.8 ha, 6.9 m) and Green Lake (113.6×10^4 m^3, 12.6 ha, 9.0 m) have similar volumes, surface areas, and mean depths (Northcote & Hall, 1983). Although the dimensions of the lakes are comparable, water column redox conditions are strikingly different. The Mahoney Lake monimolimnion persistently contains dissolved sulfide, whereas bottom waters in Green Lake are perennially saturated with oxygen. The similar physical features suggest other factors are responsible for meromixis in Mahoney Lake. Northcote and Hall (1983)

proposed that the hills surrounding Mahoney shelter the lake from prevailing winds and thus wind-blown mixing. In contrast, Green Lake is exposed to strong northeasterly winds that routinely mix the water column (Ward et al., 1989; Ward et al., 1990).

Sediments and pore waters were extracted from Cores 2 and 3 collected within the euxinic water mass from the deepest portion of Mahoney Lake in September 2006; Core 9 was collected at the same time along the oxic margin above the chemocline (Figure 1). Water column samples were also collected from Green Lake as a reference for oxic conditions in a saline lake. Water column samples were collected from Mahoney Lake in September 2006 and July 2008. During the later trip, water was also sampled from a shallow pond (< 1 m) in the hills to the west ('ML pond') and from Sleeping Lake to the east (Figure 1).

Water column sampling

Photosynthetically available radiation was measured with a spherical light sensor (LI-193, LI-COR Environmental, Lincoln, NE, USA). Light attenuation above and below the microbial plate was determined according to Beer-Bouguer's Law:

$$I_z = I_o e^{-kz}, \quad (1)$$

where radiation incident at depth (I_z) is proportional to the light intensity from the surface (I_o) and the extinction coefficient (k) at a given depth (z). Turbidity was measured as an indication of water clarity and microbial biomass (2020c Turbidimeter, LaMotte Company, Chestertown, MD, USA). Water column pH, temperature, specific conductivity, and dissolved oxygen profiles were

208 measured *in situ* with a handheld meter and probe (Quanta, Hydrolab, Loveland, CO, USA).
209 Water column samples were collected with a battery-powered pump at depth intervals of 10 to
210 100 cm. High-resolution samples were also collected in the water column with a syringe sampler
211 that allowed sampling at fixed intervals (10 cm) with minimal disturbance of the chemocline.
212 The dissolved oxygen meter was attached to the base of the syringe sampler, and the position of
213 the syringe ports relative to the location of the oxic-anoxic interface was determined from the
214 oxygen concentrations measured *in situ* and the known distance between the syringes and the
215 probe. Samples from the water column collected for sulfide analysis were preserved with 3%
216 (wt./volume) zinc acetate solution for concentration determinations or precipitated with cadmium
217 acetate for sulfur isotope analysis. A subset of samples from the water column was taken for
218 elemental sulfur were filtered onto 0.2 μm polyestersulfone filters (Millipore) under nitrogen
219 atmosphere and stored frozen at -20°C.
220
221 ***Sediments and pore waters***
222 Lake sediments were collected with a modified gravity-piston corer (Fisher et al., 1992).
223 Sediment cores were capped, sealed, and taken to the field laboratory for processing within hours
224 of collection. Sediments were sectioned and extruded in a nitrogen-filled glovebag. Surfaces of
225 the whole-round mud samples in contact with the core liner were scrapped to remove potential
226 lake water contamination and to minimize the effects of smearing. Pore waters were extracted by
227 centrifugation and filtered through 0.2 μm syringe filters. Pore water splits were preserved for
228 sulfide concentrations with 3% (wt./volume) zinc acetate solution or precipitated with cadmium
229 acetate for sulfur isotope analysis. Sediment samples were then purged with nitrogen gas, frozen,
230 and transported to our labs in Riverside for subsequent analyses.

231

232 ***Analytical***

233 Sedimentary sulfides were extracted from wet, freshly thawed sediment by sequential
234 extractions. Water content was determined by weighing separate sediment splits before and after
235 drying and corrected for mass addition from salts that precipitated during sample drying in order
236 to present the data as wt.% on a dry sediment basis. Acid volatile sulfides (AVS; FeS) were
237 extracted with a room temperature solution of 6N HCl and 15% (wt./volume) stannous chloride
238 (Chanton & Martens, 1985; Cornwell & Morse, 1987). The extractant was subsequently
239 separated from the sediment by filtration onto a glass fiber filter, and chromium reducible sulfide
240 (CRS; pyrite and elemental sulfur) was then liberated from the filtered residue by reaction with a
241 solution of boiling 1M chromous chloride and concentrated HCl (Canfield et al., 1986).
242 Chromium reducible sulfide (dominantly pyrite in this case) was also extracted from a
243 greenstone rock sample collected within the catchment. Hydrogen sulfide evolved from these
244 distillations was trapped in 3% zinc acetate solution for concentration measurements by
245 iodometric titration or precipitated as Ag_2S in a solution of 3% silver nitrate and 10% ammonium
246 hydroxide for sulfur isotope analysis (wt./volume).

247

248 The degree of sulfurization (DOS) (Boesen & Postma, 1988; Raiswell et al., 1994) was
249 determined according to the relationship:

250

251 $$\mathrm{DOS} = \frac{\mathrm{Fe_{AVS}} + \mathrm{Fe_{py}}}{\mathrm{Fe_{AVS}} + \mathrm{Fe_{py}} + \mathrm{Fe_{HCl}}} \quad (2)$$

252 where Fe_{AVS} and Fe_{py} are the concentrations of AVS-iron and pyrite-iron calculated from
253 extracted concentrations of AVS-sulfur and pyrite-sulfur and assuming the respective

stoichiometries of FeS and FeS_2. Reactive iron, Fe_{HCl}, was extracted from dried sediment with boiling 12N HCl (Berner, 1970; Raiswell et al., 1988), and extractable iron concentrations were measured by the Ferrozine colorimetric method (Stookey, 1970). High DOS values, approaching unity in extreme cases, indicate formation and accumulation of sedimentary iron-sulfide minerals under euxinic (iron-limited) conditions.

Dissolved sulfide in the water column and pore waters was preserved in the field with zinc acetate or cadmium acetate followed by centrifugation, and aliquots of the supernatant were isolated for determining chloride and sulfate concentrations. Dissolved sulfide concentrations were determined colorimetrically (Cline, 1969). Sulfate concentrations were measured gravimetrically or as dissolved S by ICP-MS with Xe as the collision cell gas (Agilent 7400 Quadrupole ICP-MS). Sulfate concentrations determined by either method agreed within ±5%. Chloride concentrations were measured by titration (DP-957M Digital Chloridometer, Haake Buchler Instruments Inc., Saddlebrook, NJ, USA). Supernatant splits were also taken for sulfur and oxygen isotope analysis of sulfate. The addition of zinc acetate to water column and pore water samples caused the dissolved sulfide to precipitate immediately and thus precluded secondary sulfate contributions from sulfide oxidation. Sulfate was precipitated as $BaSO_4$ by addition of saturated $BaCl_2$ solution (250 g/L) followed by brief acidification (4N HCl) to remove carbonates, rinsing to neutral pH, and drying. Elemental sulfur was extracted from filters collected from the water column onto copper turnings using hexane and sonication, which was subsequently liberated by chromium reduction (Canfield et al., 1986) and trapped in silver nitrate. Sulfides fixed as CdS in the field were rinsed with deionized water and reprecipitated as Ag_2S by addition of 3% silver nitrate and 10% ammonium hydroxide (wt./volume). Precipitates

277 of sulfate ($BaSO_4$) and sulfide (Ag_2S) derived from sediment extracts or dissolved species were
278 dried and homogenized with agate mortar and pestle prior to isotopic analysis.
279
280 Isotope compositions were expressed according to the equation:
281
282 $$\delta\,{}^{x}\mathrm{E} = \left[\left(R_{\mathrm{sample}}/R_{\mathrm{standard}}\right)\text{-}1\right] \times 1000 \quad (3)$$
283
284 where ^{x}E is the given isotope (^{2}H, ^{18}O, or ^{34}S), and R is the ^{2}H/^{1}H, ^{18}O/^{16}O, or ^{34}S/^{32}S ratio
285 relative to the respective international standards for H and O (V-SMOW), and S (V-CDT).
286 Water column samples were distilled prior to hydrogen and oxygen isotope analysis (West et al.,
287 2006) and analyzed at the Purdue Stable Isotope Facility, Purdue University, using a Thermo-
288 Chemical Elemental Analyzer coupled with a stable isotope ratio mass spectrometer (TCEA-
289 IRMS; Delta V; ThermoElectron, Bremen, Germany). Analytical precision was better than
290 ±0.1‰ for δD_{H2O} and ±0.2‰ for $\delta^{18}O_{H2O}$. Sulfur isotope ratios of the sulfide phases and sulfur
291 and oxygen isotopes of sulfate were analyzed on a Delta V Plus IRMS (ThermoElectron,
292 Bremen, Germany) at the Department of Earth Sciences, University of California, Riverside.
293 Samples precipitated as either Ag_2S or $BaSO_4$ were weighed into tin capsules with a ten-fold
294 excess of V_2O_5 for a final sample mass of ~50 μg-S and combusted on an ECS elemental
295 analyzer (Costech Analytical, USA) coupled under continuous flow to the IRMS. $\delta^{34}S_{BaSO4}$
296 values were normalized to international standards NBS-127 (21.1‰), IAEA SO-5 (0.49‰), and
297 IAEA SO-6 (-34.05‰). Values for $\delta^{34}S_{Ag2S}$ were normalized to IAEA standards S1 (-0.3‰), S2
298 (22.65‰), and S3 (-32.5‰). $\delta^{18}O_{SO4}$ values were determined by TCEA-IRMS and calibrated
299 against NBS-127 (8.7‰), IAEA SO-5 (12.0‰), and IAEA SO-6 (-11.0‰). Reproducibility of

300 standard reference materials and sample replicates were ±0.2‰ for $\delta^{34}S$ and ±0.4‰ for $\delta^{18}O_{SO4}$.

301

302 ***Sulfate reduction models of $\delta^{34}S_{SO4}$ and $\delta^{18}O_{SO4}$***

303 Linear and non-linear regressions of $\delta^{18}O_{SO4}$ and $\delta^{34}S_{SO4}$ (Böttcher et al., 1998; Brunner et al.,
304 2005; Brunner et al., 2012; Antler et al., 2013) can provide insight into the relative rates of
305 sulfate reduction and the extent of back reaction that occurs during intracellular cycling of sulfur
306 intermediates. We use models, developed by Antler et al., (2013), that couple the sulfur and
307 oxygen isotope (kinetic and equilibrium) fractionations that occur during sulfate reduction to
308 provide a framework for interpreting the isotopic variation observed in Mahoney Lake. Antler et
309 al. (2013) defined two trends that describe linear (Trend A) and curvilinear (Trend B) responses
310 in $\delta^{18}O$-$\delta^{34}S$ isotope space (Figure 7A). We briefly describe their models here, but full details
311 and explanations of their assumptions are provided in Antler et al. (2013).

312

313 The models are sensitive to the ratio of the forward and backward fluxes (X = b/f) of sulfur
314 within the cell and the associated kinetic isotope fractions (ε) that occur during three steps in the
315 sulfate reduction network. The steps include sulfate uptake into the cell (X_1; $\varepsilon^{34}S$ = -3‰; $\varepsilon^{18}O$ = -
316 0.75‰), the reduction of adenosine 5'-phosphosulfate (APS) to sulfite (X_2; $\varepsilon^{34}S$ = 25‰; $\varepsilon^{18}O$ =
317 6.25‰), and the reduction of sulfite to sulfide (X_3; $\varepsilon^{34}S$ = 25‰; $\varepsilon^{18}O$ = 6.25‰) (Mizutani &
318 Rafter, 1969; Rees, 1973; Antler et al., 2013). The $\delta^{18}O$-$\delta^{34}S$ isotope pattern is linear (Trend A)
319 when there is no reverse flux of sulfur ($X_1 \cdot X_3 = 0$) according to the equation,

320

$$\delta^{18}O_{SO_{4(t)}} = \frac{\varepsilon^{18}O_{total}}{\varepsilon^{34}S_{total}} \cdot \left(\delta^{34}S_{SO_{4(t)}} - \delta^{34}S_{SO_{4(o)}}\right) + \delta^{18}O_{SO_{4(o)}} \cdot \quad (4)$$

321

322

The relationship is non-linear (Trend B) when intracellular recycling (back reaction) occurs during sulfate reduction ($0 < X_1 \cdot X_3 < 1$) where,

$$\delta^{18}O_{SO_{4(t)}} = \delta^{18}O_{SO_{4(A.E.)}} - \exp\left(-\theta_0 \cdot \frac{\delta^{34}S_{SO_{4(t)}} - \delta^{34}S_{SO_{4(o)}}}{\varepsilon^{34}S_{total}}\right) \cdot \left(\delta^{18}O_{SO_{4(A.E.)}} - \delta^{18}O_{SO_{4(o)}}\right). \quad (5)$$

The residual sulfate ($\delta^{18}O_{SO_{4(t)}}$) produced by the process of microbial sulfate reduction can thus be a linear function (Equation 4) of the total fractionation factors for sulfur and oxygen isotopes ($\varepsilon^{34}S_{total}$ and $\varepsilon^{18}O_{total}$), the sulfur isotope composition of residual sulfate ($\delta^{34}S_{SO_{4(t)}}$), the initial isotopic compositions of sulfate ($\delta^{34}S_{SO_{4(o)}}$ and $\delta^{18}O_{SO_{4(o)}}$). The oxygen isotope composition of sulfate at apparent equilibrium ($\delta^{18}O_{SO_{4(A.E.)}}$) and the relationship ($\theta_0$) between oxygen isotope exchange and the rate of sulfate reduction [where $\theta_0 = (X_1 \cdot X_3)/(1 - X_1 \cdot X_3)$] become critical parameters in non-linear datasets (Equation 5).

3. Results

Isotopic composition ($\delta^{34}S_{SO4}$, $\delta^{18}O_{SO4}$, $\delta^{18}O_{H2O}$) of surface waters

The $\delta^{34}S_{SO4}$ (22.1‰) and $\delta^{18}O_{SO4}$ (16.7‰) values of surface-water sulfate collected from the upper meter of the Mahoney Lake water column resembled dissolved sulfate values in the ML pond (Figure 1). In contrast, the isotopic composition of sulfate in Green Lake ($\delta^{34}S_{SO4}$ = 1.4‰ and $\delta^{18}O_{SO4}$ = 10.8‰) and Sleeping Lake ($\delta^{34}S_{SO4}$ = 1.6‰ and $\delta^{18}O_{SO4}$ = 10.9‰) were relatively depleted in ^{34}S and ^{18}O. The low $\delta^{34}S$ values of Green and Sleeping lakes were consistent with a greenstone sample collected to the east of Mahoney Lake ($\delta^{34}S_{Greenstone}$ = 0.8‰).

Surface waters collected from shallow domestic wells and numerous lakes in the area exhibit high $\delta^{18}O$ and δD driven by intense rates of evaporation within the arid Okanagan Valley (Figure 2 and references cited therein). Vertical profiles exhibit little variation within the mixolimnion ($\delta^{18}O_{H2O} \approx 0.8‰$) and decrease abruptly across the chemocline to lower values ($\delta^{18}O_{H2O} \approx$ -1.5‰) within the monomolimnion (Figure 2; Table 1). The slope of the local evaporation line (4.7) is consistent with evaporation trends observed in hydrologically closed northern latitude lakes (Gibson et al., 2002; Gibson et al., 2005) (Figure 2).

Water column chemistry

Representative profiles of water column dissolved oxygen, specific conductivity, temperature, and pH demonstrate the sharp redox contrast between Green Lake and Mahoney Lake (Figure 3A). Green Lake is well mixed to a depth of 9 m and oxygenated throughout the water column. In contrast, dissolved oxygen in Mahoney Lake is consumed within 7 m water depth. The specific conductivity of Mahoney surface waters (~ 43 mS/cm) is elevated relative to Green Lake salinities by an order of magnitude. Conductivity increased 1.5-fold within the monomolimnion of Mahoney. Water temperatures below the chemocline are isothermal (~ 9ºC) and remain highly stable relative to inter-annual fluctuations in surface water temperatures (Northcote & Halsey, 1969; Northcote & Hall, 1990; Ward et al., 1990).

Redox conditions in Mahoney Lake in September 2006 were equivalent to observations made in July 2008 (compare Figure 3A and 3B). The chemocline was positioned at approximately 7 m

366 during both years. The maximum sulfide concentrations in the water column were extremely
367 high, ranging from 36 mM (2006) to 41 mM (2008).
368
369 The plate of purple sulfur bacteria was positioned at the pycnocline where sunlight enters sulfidic
370 water (Figure 3B). Extinction coefficients increased from the mixolimnion (k = 0.400) to the
371 quantitative absorption of sunlight below the plate (k = 3.347) such that less than 0.01% of
372 incident light penetrated below 8 m water depth. Turbidity is highest within the microbial plate
373 (Figure 3B). Abundant levels of polysulfides and elemental sulfur (Overmann et al., 1996;
374 Overmann, 1997) likely contribute to the yellow color of the monomolimnion.
375
376 Respective chloride and sulfate concentrations averaged 57.7 ± 1.7 mM and 341.8 ± 20.1 mM in
377 the upper 5 m of the mixolinion (Figure 4) of Mahoney Lake. Chloride concentrations increased
378 to approximately 70 mM in the monimolimnion; bottom-water sulfate concentrations were ~500
379 mM. Molar SO_4/Cl ratios also increased within the bottom waters. Vertical profiles collected
380 during the two field studies were broadly consistent, with the exception of maxima for sulfate
381 and chloride concentrations positioned above the chemocline at 6.3 to 6.6 m water depth (2006,
382 Figure 4), respectively, coincident with a localized decrease in dissolved oxygen concentrations.
383
384 ***Isotopic composition ($\delta^{34}S_{H2S}$, $\delta^{34}S_{SO4}$, $\delta^{18}O_{SO4}$) of the Mahoney Lake water column***
385 The $\delta^{34}S_{SO4}$ and $\delta^{18}O_{SO4}$ values for samples collected in September 2006 and July 2008 were
386 similar (Table 1). Relative to the surface, dissolved sulfate exhibited rapid enrichments in ^{34}S and
387 ^{18}O across the chemocline and remained fairly constant down to the sediment-water interface
388 (Figure 4). $\delta^{34}S_{SO4}$ values within the mixolimnion averaged 22.1 ± 0.2‰ (n = 34) and increased

389 to 27.7 ± 0.5‰ (n = 16) within 0.5 m below the chemocline. $\delta^{18}O_{SO4}$ values averaged 17.1 ±
390 0.4‰ (n = 34) above the chemocline and increased to 20.0 ± 0.6‰ (n = 34) within the
391 monimolimnion (7.5 m to bottom). The ~5.6‰ increase in $\delta^{34}S_{SO4}$ and ~2.9‰ increase in
392 $\delta^{18}O_{SO4}$ across the chemocline is consistent with the process of microbial sulfate reduction;
393 however, the sulfate concentrations also increased in the bottom waters (Figure 4), even when
394 normalized to a conservative element such as chloride. The expected distillation pattern of
395 sulfate consumption and increasing isotope composition of residual sulfate was not observed,
396 and therefore precluded the calculation of fractionation factors using Rayleigh-type equations
397 (e.g., Mariotti et al., 1981).
398
399 The $\delta^{34}S$ value of dissolved sulfide in the water column was -14.8‰ at the oxic-anoxic interface
400 and decreased to a minimum value of -25.1‰ one meter below the chemocline (8 m, September
401 2006, Figure 4). The isotopic composition of dissolved sulfide then increased progressively with
402 depth by ~2‰ above the sediment-water interface (12 to 13 m depth). The average isotopic
403 offset at the chemocline ($\Delta^{34}S_{SO4\text{-}H2S}$ = 37.1‰), calculated as the difference between $\delta^{34}S_{SO4}$ and
404 $\delta^{34}S_{H2S}$, increased with depth until 7.5 m ($\Delta^{34}S_{SO4\text{-}H2S}$ = 51‰), where it maintained a constant
405 offset throughout the lower water column. The apparent fractionations are consistent with
406 previous results of Overmann et al. (1996), which ranged from 49.4 to 55.5‰.
407
408 ***Sedimentary sulfur and pore waters in Mahoney Lake***
409 Solid-phase sulfur concentrations in sediments collected below the euxinic water mass (Cores 2
410 and 3) were marginally higher than the sulfur content in a core collected above the chemocline
411 (Core 9) (Table 2; Figure 5A). In Cores 2 and 3, AVS averaged 0.26 ± 0.06 wt.% (n = 29),

412 compared to Core 9 concentrations of 0.12 ± 0.07 wt.% (n = 15). Downcore AVS was generally
413 invariant within the anoxic cores relative to the subtle increase in concentrations toward the
414 terminal depth of the oxic core. Pyrite-S concentrations (CRS) were higher in the anoxic cores
415 (0.32 ± 0.2 wt.%, n = 19) relative to the oxic core (0.04 ± 0.01 wt.%, n= 14). There was a
416 distinct pyrite maximum at 5.5 cm, followed by a near-linear decrease in concentrations within
417 Core 2. The high degree of sulfurization (DOS > 0.7) within Cores 2 and 3 positioned below the
418 monimolimnion, including high values right at the sediment-water interface, is consistent with
419 pyrite that formed in the euxinic water column or at the sediment-water interface (i.e., syngenetic
420 pyrite). Mineral sulfide formation increased with sediment depth in oxic Core 9. Coincident with
421 this increase, the DOS generally increased from a surficial value of 0.62 to 0.88 at the base of the
422 core but with a distinct minimum of 0.28 at 9 cm. The high DOS values in Core 9 suggest past
423 euxinic conditions at this presently oxic site (see discussion below).
424
425 The concentrations and isotope values of sulfate in pore waters (Table 3) extracted from cores
426 collected above and below the current position of the chemocline reflect the chemical
427 composition of the overlying water. Specifically, interstitial sulfate concentrations in Cores 2
428 and 3 (451.6 ± 27 mM) were similar to sulfate levels within the anoxic water column (426.7 ± 53
429 mM). Likewise, within the oxic portion of the lake, Core 9 pore waters (300.1 ± 7 mM) were
430 similar to those within the mixolimnion (353.8 ± 44 mM). The isotopic composition of pore
431 water sulfate was nearly identical to the respective $\delta^{34}S_{SO4}$ and $\delta^{18}O_{SO4}$ of the oxic and anoxic
432 bottom waters (Figure 5B). Although pore water sulfide concentrations were highly variable
433 within Cores 2 and 3 (14.63 ± 7 mM), dissolved sulfide levels within Core 9 (1.66 ± 0.4 mM)
434 were uniform and an order of magnitude lower than those within the euxinic cores (Table 3). The

435 $\delta^{34}S$ of pore water sulfide from Cores 2 and 3 (-22.1 ± 2‰) was consistent with that of bottom-
436 water sulfide (-22.5 ± 2.8‰) (Figure 5B). Relative to the anoxic bottom waters, however, the
437 isotopic composition of dissolved sulfide in Core 9 pore waters tended toward lower $\delta^{34}S$ values,
438 ranging from -17.9 to -36.0‰.
439
440 **4. Discussion**
441 ***Stable isotope spatial patterns and the Mahoney Lake sulfur supply***
442 The sulfur inventory of Mahoney Lake is exceptionally large, even when compared to both
443 modern and ancient seawater. Water column sulfide (>30 mM) is two orders of magnitude higher
444 than concentrations measured in the deep waters of the Black Sea (Neretin et al., 2003), and the
445 sulfate pool (>300 mM) is tenfold greater than modern seawater. Although the source of sulfur
446 has yet to be directly analyzed, Mahoney Lake sulfate is thought to be derived from the chemical
447 dissolution of alkaline lavas (Northcote & Hall, 1983) in the western extent of the catchment
448 (Marron Formation, Figure 1). The $\delta^{34}S$ for such a source should fall near 0‰, but intriguingly,
449 the isotopic composition of sulfate in Mahoney Lake ($\delta^{34}S_{SO4} \approx 22$‰) is similar to that of
450 modern seawater ($\delta^{34}S_{SO4} = 21$‰) (Rees, 1978). Equivalent values ($\delta^{34}S_{SO4} = 19.9$‰) were
451 reported for drill-hole fluids (Michel et al., 2002) that infiltrate the White Lake Formation
452 (composed of shale, sandstones, and volcanic conglomerates) 5 km to the northwest of the study
453 area (Church, 2002).
454
455 The fault beneath both lakes (Figure 1) is a potential pathway for fluid flow into the catchment
456 given that the overall geology of this region is highly fractured and favorable to basin-wide
457 circulation of groundwater and hydrothermal fluids (Michels et al. 2002). Geothermal fluids

458 common to the region have characteristically high $\delta^{18}O_{H2O}$ (Magaritz & Taylor, 1986; Criss et
459 al., 1991) (Figure 2, inset) and are unlikely sources of fluids because the lake water is very
460 similar to meteoric inputs (Figure 2, LMWL). Long-term monitoring of lake levels further
461 confirm that groundwater inflow is the dominant supply of water into Mahoney Lake (Northcote
462 & Hall, 2000).
463
464 The similarity between $\delta^{34}S$ of the greenstone (0.8‰) and Sleeping Lake sulfate (1.6‰) suggests
465 a sulfur source distinct from Mahoney Lake and Mahoney pond, which are both 20‰ higher and
466 located less than 1 km away (Figure 1). The high $\delta^{34}S_{SO4}$ values in Mahoney Lake and the
467 adjacent pond were derived either from a sulfur source from the western extent of the catchment
468 or from a precursor sulfate similar to that of Sleeping Lake but that was heavily overprinted by
469 isotopic fractionation during dissimilatory sulfate reduction. The Mahoney pond, perched above
470 the lake, was observed to vary from a dry salt bed (2006) to a shallow pond (2008) during our
471 two visits. Driving the sulfate pool to higher $\delta^{34}S$ and $\delta^{18}O$ in both an ephemeral pond and a
472 persistent lake would require similar redox conditions and organic matter availability. However,
473 climatic controls in the region suggest that the Mahoney pond likely remained dry for extended
474 periods relative to the more stable water balance of Mahoney Lake. As such, sulfate pools in the
475 two settings would evolve on different timescales and under different conditions, and therefore
476 dissimilar $\delta^{34}S$ and $\delta^{18}O$ values should result. We are left with the likelihood that sulfate-rich
477 waters in Mahoney Lake are delivered from weathering products derived from formations
478 located to the west of the fault that bisects the catchment.
479
480 ***Water column stable isotope patterns***

Our study captured the steady-state isotopic variability ($\delta^{34}S_{SO4}$, $\delta^{18}O_{SO4}$, and $\delta^{34}S_{H2S}$) of microbial processes within the Mahoney Lake water column during late summer to early fall. A turbidity maximum (Figure 3B) that coincides with the purple layer, the first appearance of dissolved sulfide, and near complete light attenuation, is proxy evidence for increased microbial biomass at the oxic-anoxic interface. The microbial plate (at 7 m) absorbs available light almost completely (Figure 3B), thus inhibiting further autotrophic production deeper in the water column.

Microbial activity within the plate follows a seasonal pattern marked by peak productivity by purple sulfur bacteria during the late spring through early summer (Overmann et al., 1996). Through concomitant degradation of this biomass, sulfate reduction in the plate also becomes quantitatively important in late spring but extends through early fall (Overmann et al., 1991; Overmann et al., 1996). Primary production by purple sulfur bacteria is most intense at the top of the plate and is regulated by incoming solar radiation and the upward flux of dissolved sulfide transported from the monimolimnion (Overmann et al., 1991; Overmann et al., 1996). Mass balance estimates (Overmann et al., 1994; Overmann et al., 1996) as well as metagenomic data (Hamilton et al., 2014) indicate that chemoautotrophy is a significant sulfide oxidation pathway within the plate—in addition to anoxygenic photosynthesis.

Comparison of rates of sulfate reduction (i.e., sulfide production) and anoxygenic photosynthetic productivity suggests that sulfate reduction is carbon-limited (Overmann et al., 1991; Overmann et al., 1996; Hamilton et al., 2014). Measured rates of carbon fixation and heterotrophic activity reveal that the carbon demand by sulfate reducers is greater than the amount of carbon fixed

504 during the summer; however, annual fixation rates (33.5 g C m^{-2} yr^{-1}) are sufficient to satisfy the
505 demand of sulfate reducers within the microbial plate (22.5 g C m^{-2} yr^{-1}) (Overmann et al., 1996).
506 Details of the extant microbial community were further refined by a recent study of 16s rRNA
507 genes, which demonstrated that the Mahoney sulfur cycle is mediated by phototrophic sulfide
508 oxidizers and oxidation of sulfide and intermediates by Epsilonproteobacteria and
509 Deltaproteobacteria at the chemocline (7m) (Klepac-Ceraj et al., 2012). Microbiological
510 evidence was also observed for sulfate reducers throughout the monimolimnion and within the
511 sediments (Klepac-Ceraj et al., 2012; Hamilton et al., 2014). Although direct measurements of
512 sulfate reduction rates and biomass enumerations are needed to determine the relative roles of
513 these microorganisms, the genetic data confirm the activity of sulfate reducers within the lower
514 water column and the sediments.
515
516 The co-occurring processes of microbial sulfide production and sulfide oxidation provide a
517 unique opportunity to study sulfur redox chemistry in a highly sulfidic natural system. Isotope
518 patterns of sulfate and sulfide indicate active sulfate reduction at the oxic-anoxic interface in the
519 water column (Figure 4). In our study, rapid increases in $\delta^{34}S_{SO4}$ (~5‰) and $\delta^{18}O_{SO4}$ (~3‰)
520 stabilized to constant values within the first 0.5 m below the chemocline. The relatively uniform
521 sulfur isotope values for the sulfide in the deeper monimolimnion also increased at the
522 chemocline by 7 to 9.5‰. These isotope patterns are best explained by a combination of
523 fractionations that occur during sulfate reduction and sulfide oxidation.
524
525 Initial experiments with laboratory cultures suggested that the isotope effect that accompanies
526 dissimilatory sulfate reduction produces offsets between sulfate and sulfide ($\Delta^{34}S_{SO4\text{-}H2S}$) of up to

527 ~46‰ (Kaplan & Rittenberg, 1964b; Chambers et al., 1975) and that these results may reflect the
528 maximum fractionations possible by sulfate reduction alone in the lab or natural settings
529 (Canfield, 2001). However, recent culture experiments (Sim et al., 2011; Leavitt et al., 2013)
530 and work in natural environments (Canfield et al., 2010) demonstrate fractionations of 60-70‰
531 for sulfate reduction alone. Metabolic models for sulfate uptake followed by a series of
532 enzymatic reduction steps within the cell that reduce sulfite and ultimately excrete sulfide (Rees,
533 1973) may under-predict the magnitude of fractionation found in the natural environment (65-
534 70‰) (Rudnicki et al., 2001; Wortmann et al., 2001). Brunner and Bernasconi (2005) reassessed
535 biochemical pathways and fractionation effects that accompany reduction of sulfite to sulfide via
536 the trithionate pathway and extended the potential fractionations up to 70‰. Network reaction
537 models that incorporated multiple sulfur isotopes (^{32}S, ^{33}S, ^{34}S, and ^{36}S) (Farquhar et al., 2003;
538 Farquhar et al., 2007; Johnston et al., 2007) improved the ability to model internal sulfur
539 transformations, yet the relevant consequences of the enzyme dissimilatory sulfite reductase,
540 which catalyzes the reduction of sulfite to sulfide, remain to be fully explored and understood
541 (Bradley et al., 2011). The models discussed above establish the theoretical constraints on sulfur
542 isotope effects during sulfate reduction, but the full expression of $\delta^{34}S$ fractionation may also
543 reflect environmental variables such as sulfate reduction rates (Kaplan & Rittenberg, 1964a;
544 Kemp & Thode, 1968), carbon substrate (Aharon & Fu, 2000; Bolliger et al., 2001; Detmers et
545 al., 2001), environmental conditions and microbial community structure (Brüchert et al., 2001;
546 Detmers et al., 2001), and the size of the sulfate reservoir (Harrison & Thode, 1958; Habicht et
547 al., 2002).
548

549 The oxidative sulfur cycle may further expand the isotopic difference between sulfate and
550 sulfide. The presence of dissolved oxygen and purple sulfur bacteria at the redox interface of
551 Mahoney Lake promotes abiotically and biotically mediated sulfide oxidation. However, sulfur
552 isotope effects associated with sulfide oxidation are small (±5‰). For example, direct chemical
553 oxidation of aqueous sulfide with molecular oxygen can increase $\delta^{34}S_{H2S}$ by 5‰ (Fry et al.,
554 1988b), and purple sulfur bacteria typically produce residual $\delta^{34}S_{H2S}$ that is 2-5‰ lower than the
555 product sulfate (Fry et al., 1984; Fry, 1986; Fry et al., 1988a; Zerkle et al., 2009; Zerkle et al.,
556 2010; Brabec et al., 2012). Much larger fractionations are expected for sulfur disproportionation.
557 For example, the simultaneous oxidation and reduction of sulfite produces ^{34}S-enriched sulfate
558 (7-12‰) and ^{34}S-depleted sulfide (20-37‰) (Habicht et al., 1998). Combined transformations of
559 reduction, reooxidation, and disproportionation have been invoked to explain large net isotopic
560 offsets between sulfate and sulfide (Canfield & Thamdrup, 1994), particularly if the redox cycle
561 is repeated multiple times.
562
563 Chemical (Zhang & Millero, 1994) and microbial (Zopfi et al., 2001) sulfide oxidation at the
564 chemocline generates intermediate sulfur compounds (S^0, SO_3^{2-}, $S_2O_3^{2-}$) that can undergo
565 disproportionation; however, biological and environmental conditions in Mahoney Lake
566 potentially preclude or limit disproportionation to a very narrow zone within the uppermost
567 portion of the chemocline. For example, purple sulfur bacteria oxidize sulfide directly to
568 elemental sulfur, producing only very low levels of thiosulfate in Mahoney Lake (<1 – 20 μM)
569 — levels that can inhibit thiosulfate disproportionation (Overmann et al., 1996). Furthermore, the
570 high sulfide levels within the monimolimnion, well in excess of the sulfide tolerance (~1 mM)
571 for either elemental sulfur or thiosulfate disproportionators (Thamdrup et al., 1993), likely

restricts disproportionators to the upper-cm of the chemocline. That said, the spatial resolution of our sampling methods (10 to 100 cm) might not capture the microbial signatures or specific chemical conditions at the top of the sulfide interface where sulfur disproportionating organisms could be active.

The microbial process of sulfate reduction and associated rates appear to be to have the greatest influence on the isotopic patterns observed in this hyper-euxinic lake. The apparent fractionation between sulfate and sulfide (37.1 to 39.5‰) at the chemocline increased to 51‰ in water layers below the chemocline and remained fairly uniform throughout the monimolimnion (Figure 6). Consistent with previous results from Mahoney that ranged from 49 to 55‰ for coeval sulfate and sulfide sampled at the chemocline and 12 m water depth (Overmann et al., 1996), our data expand the vertical resolution and capture the increase in $\delta^{34}S_{H2S}$ values at the chemocline. The isotopic offset between oxidized and reduced sulfur in Mahoney Lake is similar to the large fractionations reported for euxinic marine water columns such as in the Black Sea, Cariaco Basin, Framvaren Fjord, Mariager Fjord, and the Orca Basin (Sweeney & Kaplan, 1980; Sheu et al., 1988; Fry et al., 1991; Mandernack et al., 2003; Neretin et al., 2003; Sørensen & Canfield, 2004; Li et al., 2010), as well as euxinic lakes such as Lake Cadagno, Crawford Lake, and Fayetteville Green Lake (Deevey et al., 1963; Fry, 1986; Dickman & Thode, 1990; Canfield et al., 2010; Zerkle et al., 2010). Mahoney Lake has the highest concentrations of dissolved sulfide (>30 mM) and sulfate (> 300 mM) among these stratified water bodies. The large, effectively infinite sulfate reservoir in Mahoney Lake would preclude significant reservoir effects during sulfate reduction. When all these observations are considered, our favored interpretation is that large fractionations are dominantly instantaneous, occurring via sulfate reduction alone without

595 contributions from disproportionation in the sediment and water column. For these reasons,
596 sulfate reduction exerts the greatest control on $\delta^{34}S$ fractionation in Mahoney Lake.
597
598 Paired $\delta^{34}S_{SO4}$ and $\delta^{18}O_{SO4}$ data offer an additional constraint on the microbial redox cycle within
599 Mahoney Lake. The low temperature and near-neutral pH of the Mahoney water column
600 measured during our studies (pH 7-9, 9-24ºC), as well as during long-term monitoring
601 (Northcote & Halsey, 1969; Northcote & Hall, 1983), suggest that sulfate-oxygen has not
602 undergone abiotic equilibrium exchange and thus records biogenic oxygen isotope effects. Under
603 anoxic conditions, sulfate-oxygen can fractionate during sulfate reduction, and the extent of
604 enrichment is controlled by kinetic isotope effects imparted during intracellular enzymatic steps
605 and/or equilibrium oxygen exchange with water. Mizutani and Rafter (1969) proposed a 1:4
606 ($\delta^{18}O_{SO4}$:$\delta^{34}S_{SO4}$ = 0.25) kinetic relationship between the $\delta^{34}S$ and $\delta^{18}O$ of sulfate based on an
607 assumption of preferential ^{16}O-bond rupture and the stoichiometry of the sulfate molecule. The
608 theoretical $\delta^{18}O_{SO4}$:$\delta^{34}S_{SO4}$ slope of 0.25 suggests the $\delta^{34}S$ and $\delta^{18}O$ of residual sulfate evolves in
609 a linear relationship during sulfate reduction; however, studies of natural samples tend to reveal a
610 curvilinear response that implies equilibrium isotope exchange regulates the oxygen isotope
611 composition of residual sulfate (Böttcher et al., 1998; Brunner et al., 2005; Brunner et al., 2012;
612 Antler et al., 2013). Culturing experiments and reactive transport models of natural samples point
613 to oxygen isotope exchange between water and metabolic intermediates (APS, AMP, and sulfite)
614 that buffers the $\delta^{18}O_{SO4}$ to a maximum value determined by the ambient $\delta^{18}O_{H2O}$ value and
615 associated fractionation factors (Mizutani & Rafter, 1973; Fritz et al., 1989; Brunner et al., 2005;
616 Knöller et al., 2006; Wortmann et al., 2007; Turchyn et al., 2010). The combined effects of
617 Rayleigh-type kinetic isotope fractionations and oxygen isotope exchange during sulfate

618 reduction thus results in non-linear $\delta^{18}O$-$\delta^{34}S$ arrays. In studies of marine pore waters, sulfate
619 approaches a plateau in $\delta^{18}O_{SO4}$, in apparent equilibrium with seawater, as $\delta^{34}S_{SO4}$ evolves
620 toward higher values (Zak et al., 1980; Böttcher et al., 1998; Blake et al., 2006; Riedinger et al.,
621 2010; Wehrmann et al., 2011; Antler et al., 2013). Empirical equations based on high
622 temperature exchange experiments between sulfate and water (Lloyd, 1968; Mizutani, 1972) and
623 quantum mechanical calculations (Zeebe, 2010) can constrain the $\delta^{18}O_{SO4}$ value in equilibrium
624 with ambient water. These relationships (Lloyd, 1968; Mizutani, 1972; Zeebe, 2010) yield
625 apparent equilibrium $\delta^{18}O_{SO4}$ values ranging between 24 to 36‰ for the temperature and isotopic
626 composition of anoxic water (about 9°C and -2‰) in Mahoney Lake. These equilibrium values
627 overestimate the observed $\delta^{18}O_{SO4}$ by 3 to 15‰.
628
629 Instead, we observe near-linear patterns of $\delta^{18}O_{SO4}$ and $\delta^{34}S_{SO4}$ in the water columns sampled in
630 fall and summer (Figure 7), which is a trend more consistent with high sulfate reduction rates
631 than equilibrium isotope exchange (Böttcher et al., 1998; Brunner & Bernasconi, 2005; Brunner
632 et al., 2012; Antler et al., 2013). The model arrays represent a range of possible solutions for the
633 internal cycling of sulfur during microbial sulfate reduction (Figure 7). Steep slopes (Figure 7A,
634 Trend B) with large changes in $\delta^{18}O_{SO4}$ relative to those in $\delta^{34}S_{SO4}$ are consistent with lower rates
635 of sulfate reduction and enhanced recycling of intracellular sulfur (Antler et al., 2013).
636 Conversely, low-angle slopes (Figure 7A, Trend A) with little change in $\delta^{18}O_{SO4}$ over large
637 changes in $\delta^{34}S_{SO4}$ are observed in systems with rapid sulfate reduction rates and minimal
638 recycling of intracellular sulfur (Antler et al., 2013).
639

In addition to the behavior in $\delta^{18}O_{SO4}$-$\delta^{34}S_{SO4}$, the extent of instantaneous fractionation between water column sulfate and sulfide lends support to our interpretation of high sulfate reduction rates in Mahoney Lake. It is well demonstrated that sulfur isotope fractionation factors are inversely proportional to the rates of sulfate reduction (Sim et al., 2011; Leavitt et al., 2013), which is in turn dependent on the availability and reactivity of organic matter (e.g., Overmann, 1997; Hamilton et al., 2014). We observed sulfide with high $\delta^{34}S$ (-14.8‰) and the smallest isotopic offset between sulfate and sulfide (37.1‰) at the chemocline (Figure 6), which may reflect the rapid rates of sulfate reduction in that portion of the water column. The increase in $\delta^{18}O_{SO4}$ and $\delta^{34}S_{SO4}$ thus depends on the localized activity of sulfate reducers. The process of microbial sulfate reduction may occur at the redoxcline in the water column, throughout the water column, and possibly in the sediments as well. The anoxic basins of the Black Sea and Cariaco Basin serve as templates for recognizing such hotspots of microbial activity. Sulfate reduction rates measured in the Black Sea revealed distinct zones of sulfate reduction within the chemocline and at the sediment-water interface (Albert et al., 1995). Volumetrically, the rates of sulfate reduction within the sediments of the Black Sea are three-fold greater than those within the water column, suggesting that much of the sulfide in the water column is delivered via diffusion from sulfate reduction in the sediments (Albert et al., 1995). Similar zones and modes of sulfide production are postulated for the Caricaco Basin (Fry et al., 1991; Li et al., 2010). The microbial diversity of Mahoney Lake suggests that sulfate reducing bacteria are distributed throughout the anoxic water column and sediments (Hamilton et al., 2014). The near-linear isotope arrays for sulfate with $\delta^{18}O_{SO4}$:$\delta^{34}S_{SO4}$ slopes ranging between 0.47 (July 2008; R^2 = 0.94) and 0.60 (September 2006; R^2 = 0.96) (Figure 7) are consistent with high sulfate reduction rates in the water column.

663

664 It is intriguing that the slope shifts from low values in the summer (Figure 7C) to higher values
665 in fall (Figure 7B). The shallower $\delta^{18}O_{SO4}$:$\delta^{34}S_{SO4}$ slope in the summer implies sulfate reduction
666 rates that are relatively higher than those in the fall. Overmann et al. (1996) observed that sulfate
667 reduction rates peak during the summer after the spring bloom of purple sulfur bacteria, and then
668 decrease in the fall as photosynthetic activity diminishes. Labile organic acids released from the
669 degradation of purple sulfur bacteria provide the primary carbon substrate mineralized by sulfate
670 reducers (Overmann et al., 1996). Previous studies demonstrate that linear $\delta^{18}O_{SO4}$:$\delta^{34}S_{SO4}$ slopes
671 are sensitive to the quantity and reactivity of organic matter mineralized during sulfate reduction
672 (Aharon & Fu, 2000; Antler et al., 2014). The change in the $\delta^{18}O_{SO4}$:$\delta^{34}S_{SO4}$ slope of residual
673 sulfate reported here thus may track the seasonal activity of sulfate reduction stimulated by the
674 localized primary productivity of anoxygenic phototrophs within the plate. Dedicated seasonal
675 sampling may capture a more robust isotopic signature of evolving sulfate reduction rates.
676 Likewise, our modeled data could be re-evaluated as separate but coupled trajectories for the
677 chemocline and deeper sulfide production within the bottom waters and surficial sediments;
678 however, the current data set lacks the spatial resolution to make this determination. The
679 potentially distinct zones and rates of reduction might be revealed within higher resolution
680 $\delta^{18}O_{SO4}$ and $\delta^{34}S_{SO4}$ data collected at the sub-cm scale.

681

682 Close inspection of the isotope variability near the chemocline does reveal that $\delta^{18}O_{SO4}$ varies
683 more than $\delta^{34}S_{SO4}$ (Figure 7A). The 2-3‰ increase in $\delta^{18}O_{SO4}$ and lack of response in $\delta^{34}S_{SO4}$
684 implies sulfate reduction and near quantitative reoxidation to sulfate (i.e., no net sulfur isotope
685 fractionation). Oxygen isotope fraction during disproportionation can be large (up to 21‰)

686 (Böttcher et al., 2001) and therefore do not agree with the smaller isotope effects observed here,
687 consistent with our earlier arguments against appreciable disproportionation. Below 7 m water
688 depth, both $\delta^{18}O_{SO4}$ and $\delta^{34}S_{SO4}$ follow a sulfate reduction trend of increasing values. Therefore,
689 although there is clear evidence for robust activity of sulfur oxidizing bacteria, the prevailing
690 process of microbial sulfate reduction masks the isotopic fingerprint.
691
692 We acknowledge that thermodynamic equilibrium can achieve large isotopic offsets (~ 75‰)
693 between sulfate and sulfide (Ohmoto & Lasaga, 1982; Chu et al., 2004; Farquhar et al., 2007;
694 Johnston et al., 2007; Leavitt et al., 2014) in the absence of biological activity. The extremely
695 high concentrations of aqueous sulfur compounds (including sulfate, sulfide, and polysulfide)
696 within our study area makes Mahoney Lake a candidate system for the consideration of abiotic
697 isotope fractionation. Equilibrium isotope exchange between sulfate-sulfide depends upon pH
698 and temperature and can equilibrate within days under acidic conditions (pH = 2) and high
699 temperature (>300°C) (Ohmoto & Lasaga, 1982). However, at normal Earth surface
700 temperatures (25°C) and neutral pH, near quantitative exchange (90%) between aqueous sulfate
701 and sulfide is exceedingly slow, taking on the order of 10^9 years (Ohmoto & Lasaga, 1982),
702 which is well in excess of the age of Mahoney Lake (10^4 years). The proposed mechanism for
703 sulfate-sulfide exchange may occur through a transient thiosulfate intermediate (Ohmoto &
704 Lasaga, 1982) or polysulfides (Chu et al., 2004); however, controlled experiments needed to
705 further constrain these processes remain to be conducted. One recent study shows that sulfur
706 isotope exchange may be possible during thiosulfate disproportionation but mass balance
707 considerations suggest that the isotope effects are kinetic (Leavitt et al., 2014). Based on the

current understanding of the sulfate-sulfide system, the isotope offsets in Mahoney Lake are thus most consistent with biologically meditated sulfur cycling.

Linking the pelagic S cycle with the sedimentary record

The large size of the sulfate and sulfide reservoir defines the isotopic composition of the pore waters within both the oxygenated (Core 9) and the anoxic (Cores 2 and 3) portions of the lake. Pore water $\delta^{34}S_{SO4}$ and $\delta^{18}O_{SO4}$ values are identical to the isotopic compositions of sulfate from the mixolimnion or the monimoliniom (Figure 5B). Relative to Core 9 collected from the oxic margin of Mahoney Lake, pore waters in Cores 2 and 3 are ^{34}S- and ^{18}O-enriched. The comparatively higher $\delta^{34}S_{SO4}$ and $\delta^{18}O_{SO4}$ are likely driven by fractionations during sulfate reduction.

$\delta^{34}S_{SO4}$ data for the water column and associated pore waters plot along mixing trajectories specific to the oxic and anoxic study sites (Figure 8A). Sulfate in the oxic water column has uniform $\delta^{34}S_{SO4}$ over a broad range of sulfate concentrations. Core 9 pore waters have $\delta^{34}S_{SO4}$ values identical to those of the mixolimnion. Sulfate in the anoxic water column becomes ^{34}S-enriched as sulfate concentrations increase with depth. Pore waters all have high sulfate concentrations with high $\delta^{34}S$ values. Mixing patterns in $\delta^{18}O_{SO4}$ (Figure 8B) show similar trends, albeit with greater scatter in the isotope data. Although the sulfate concentrations within the pore waters remain high and the sulfate isotope data follow patterns of mixing, the pore water $\delta^{34}S_{H2S}$ values in the oxic margin (Core 9) are highly variable (Figure 6) and decrease depth (Figure 5B), indicating active sulfide production within the sediments. As discussed above, the activity of sulfate reduction within the plate appears be tied to the productivity of purple sulfur

731 bacteria, this relationship does not preclude the burial of reactive organic compounds that
732 escaped oxidation in the water column.
733
734 The dissolved sulfide pool is also large within the monimolimnion and the pore waters within
735 Cores 2 and 3. Similarity between $\delta^{34}S_{H2S}$ in the water column and the pore waters suggests that
736 isotopic compositions are buffered by the large sulfide concentrations within the euxinic water
737 mass (Figure 5B). The concentrations of sedimentary dissolved sulfide, AVS, and pyrite beneath
738 the euxinic waters are appreciable relative to those in the sediments of the oxic margin. The $\delta^{34}S$
739 of pyrite, within our small errors, is the same as the composition of water column sulfide (Figure
740 5A). High DOS values (~0.8) within Cores 2 and 3 suggest water column pyrite synthesis within
741 a euxinic water column. Although the data suggest that pyrite formation is ultimately Fe limited,
742 the high DOS values also suggest that an iron enrichment mechanism perhaps like that observed
743 in the modern Black Sea (e.g., Lyons & Severmann, 2006) may be operating in the lake.
744
745 Seasonal recycling by reductive dissolution and oxidation may transport iron into the deeper lake
746 from the oxic margin; however, a benthic shallow-to-deep iron flux at the small scale of this
747 basin has yet to be described elsewhere. The low and invariant $\delta^{34}S$ of pyrite within both anoxic
748 cores further supports our interpretation of water column pyrite formation (Lyons, 1997; Lyons
749 et al., 2003). In contrast, pore water sulfide in Core 9 becomes more ^{34}S-depleted with depth, and
750 AVS accumulates with depth, implying sulfide generation in the sediments. The DOS values
751 within the upper 15 cm of the sediment column also increase down core, consistent with
752 diagenetic pyrite formation, and eventually reach high values more typical of water-column
753 pyrite formation in the euxinic part of the basin (0.8). A shoaling of the chemocline when water

754 levels were higher likely explains the down-core transition to higher DOS in the now oxic core.
755 Modern observations show the lake experiences long-term volumetric changes. Lake level has
756 dropped more than 5 m since 1961 (Northcote & Hall, 1990; Northcote & Hall, 2000; Northcote
757 & Hall, 2010). Decadal fluctuations in lake height potentially control the vertical position of the
758 chemocline and thus the expansion (when lake levels are high) or contraction (when lake levels
759 are low) of the volume of the euxinic bottom waters. The lateral displacement of the chemocline
760 from depo-center to margin, as tracked by excursions in DOS, may coincide with regional
761 drought. Shoaling events are well documented for the Black Sea (Lyons et al., 1993) and, in
762 Mahoney, are likely caused by changing lake volume.
763
764 ***Long-term stability of the chemocline***
765 The dissolved sulfide concentrations of >30 mM are considerable and represent extreme euxinic
766 conditions. Very high sulfide concentrations within the anoxic bottom waters are consistent with
767 previous reports (Northcote & Halsey, 1969; Northcote & Hall, 1983); however, we also
768 detected free sulfide at isolated depths in the mixolimnion at concentrations ranging 3 to 62 μM
769 (Table 1, Figure 3). The low but analytically detectable sulfide levels (> 2 μM) may reflect
770 sulfide released from aggregates of purple sulfur bacteria transported into the oxic surface waters
771 by wind-blown mixing. During both field trips, we observed aggregates of purple sulfur bacteria
772 floating within the mixolimnion and deposited along the shoreline. Overmann *et al*. (1994)
773 reported that the majority of purple sulfur bacteria were photosynthetically inactive during late
774 summer, and approximately 86% of the biomass was dispersed from the plate into the upper
775 water column.
776

Redox instability is part of the history of Mahoney Lake. Paleoreconstructions suggest anoxic conditions commenced with the formation of Mahoney Lake following glacial retreat 11,000 years ago. Diatom and midge sediment archives record elevated salinities (~10 g/L) throughout much of the Holocene (Heinrichs et al., 1997) and imply that aridity is a persistent feature of the regional climate. Okenone abundances indicate several purple sulfur bacteria blooms and periods of meromixis lasting approximately 1000 years (Overmann et al., 1993; Coolen & Overmann, 1998). The periodicity found in purple sulfur biomarkers is consistent with the absence of laminations during low stands and implies that wind-driven mixing destabilized the stratification (Dickman, 1985; Lowe et al., 1997).

5. Conclusions

We studied the isotope composition of sulfate and sulfide within the water column and sediments of a hyper-euxinic lake. Our analysis of surface water samples collected from four lakes located within the same catchment indicates that the sulfate in Mahoney Lake is derived from rock units in the western portion of the watershed. The sulfate (>300 mM) and sulfide (>30 mM) concentrations in the Mahoney Lake water column are extremely high and unlike sulfur inventories postulated for the Proterozoic and Archean oceans; however, the sulfide availability within the photic zone coupled within a highly active microbial community of sulfate reducing and sulfur phototrophic bacteria provide an ideal natural laboratory for studying biological processes thought to be prevalent in euxinic seas. Our data revealed that although there is clearly a very active plate of purple sulfur bacteria, the associated isotopic biosignature is completely overprinted by the relatively large sulfur and oxygen isotope fractionations associated with sulfate reducing bacteria. The seasonal $\delta^{18}O_{SO4}$-$\delta^{34}S_{SO4}$ patterns observed in water column

suggest that sulfate reduction rates (low $\delta^{18}O_{SO4}$:$\delta^{34}S_{SO4}$ slope) are high during the summer and decrease in the fall (high $\delta^{18}O_{SO4}$:$\delta^{34}S_{SO4}$ slope). The decrease in the offset between sulfate and sulfide ($\Delta^{34}S_{SO4\text{-}H2S}$ = 37‰) near the chemocline is also consistent with higher rates of sulfate reduction (and an associated decrease in fractionation at higher rates). Previous studies demonstrate that productivity of sulfate reducers is dependent upon carbon inputs from purple sulfur bacteria. Although the isotope signatures of sulfate reduction mask the relatively small isotope effects produced during sulfide oxidation, the linear correlation between $\delta^{18}O_{SO4}$ and $\delta^{34}S_{SO4}$ is potentially influenced by the primary production of anoxygenic photosynthetic bacteria. As with the water column, the $\delta^{34}S$ of sedimentary pyrite reflects the process of sulfate reduction. Estimates of the degree of sulfurization (DOS > 0.7) suggest that the deep basin sediments pyrites likely form in the water column and settle to the sediments. Although a mechanism for reactive iron delivery within a small basin such as Mahoney Lake has yet to be fully explored, the trend toward higher DOS within sediments collected from the oxic margin suggests lake level (and water availability) influences the expansion/contraction of the euxinic water mass.

As a result of strong overprinting by microbial sulfate reduction, there is not an obvious stable isotope signature for photosynthetic sulfide oxidation in Mahoney Lake that could be incorporated into the sedimentary record. In effect, the isotopic expression of sulfate reduction integrated over the entire anoxic water column and under non-sulfate-limiting conditions masks the isotopic effects of phototrophic sulfide oxidation within the $\delta^{18}O_{SO4}$-$\delta^{34}S_{SO4}$ system. However, there is clear evidence within seasonal response of $\delta^{18}O_{SO4}$-$\delta^{34}S_{SO4}$ for extensive sulfur cycling through phototrophic sulfide oxidation in Mahoney Lake, suggesting that if the difficult

task of constraining ambient $\delta^{18}O_{H2O}$ (Brabec et al., 2012) can be surmounted (through, for example, combined clumped isotope paleothermometry and $\delta^{18}O$ analysis of carbonate phases) the combined sulfur and oxygen isotope systematics of sedimentary sulfate may ultimately provide an archive of the prevalence and magnitude of photosynthetic sulfur cycling during Earth's history.

Acknowledgements

We thank BC Ministry of Environment Area Supervisors R. Gunoff and M. Weston for access to Mahoney Lake and their generous field support. S. Bates, A. Chappaz, A. Dekas, G. Druschel, D. Fike, B. Gill, J. Glass, M. McKibben, N. Planavsky, N. Riedinger, and A. Vossmeyer assisted in the field or laboratory. Hydrolabs were provided by M. Anderson UCR, and LacCore (National Lacustrine Core Facility, Department of Geology and Geophysics, University of Minnesota-Twin Cities). The manuscript benefited from helpful discussions with K. Hall, T. Northcote, C. Alpers, K. Mandernack, and J. Overmann. We also thank D. Johnston and two anonymous reviewers for their thoughtful and constructive reviews. Funding for our research was provided by NASA Exobiology and the NASA Astrobiology Institute (TL), the American Chemical Society Petroleum Research Fund (48736-ND2 to TL and WPG), and an Agouron Institute Geobiology Fellowship (WPG).

References

Aharon P, Fu B (2000) Microbial sulfate reduction rates and sulfur and oxygen isotope fractionations at oil and gas seeps in deepwater Gulf of Mexico. *Geochimica et Cosmochimica Acta,* **64**, 233-246.

847 Albert DB, Taylor C, Martens CS (1995) Sulfate reduction rates and low molecular weight fatty
848 acid concentrations in the water column and surficial sediments of the Black Sea. *Deep*
849 *Sea Research Part I: Oceanographic Research Papers,* **42**, 1239-1260.
850 Antler G, Turchyn AV, Herut B, Davies A, Rennie VC, Sivan O (2014) Sulfur and oxygen
851 isotope tracing of sulfate driven anaerobic methane oxidation in estuarine sediments.
852 *Estuarine, Coastal and Shelf Science,* **142**, 4-11.
853 Antler G, Turchyn AV, Rennie V, Herut B, Sivan O (2013) Coupled sulfur and oxygen isotope
854 insight into bacterial sulfate reduction in the natural environment. *Geochimica et*
855 *Cosmochimica Acta,* **118**, 98-117.
856 Balci N, Mayer B, Shanks Iii WC, Mandernack KW (2012) Oxygen and sulfur isotope
857 systematics of sulfate produced during abiotic and bacterial oxidation of sphalerite and
858 elemental sulfur. *Geochimica et Cosmochimica Acta,* **77**, 335-351.
859 Balci N, Shanks WC, Iii, Mayer B, Mandernack KW (2007) Oxygen and sulfur isotope
860 systematics of sulfate produced by bacterial and abiotic oxidation of pyrite. *Geochimica*
861 *et Cosmochimica Acta,* **71**, 3796-3811.
862 Bekker A, Holland HD, Wang PL, Rumble D, Stein HJ, Hannah JL, Coetzee LL, Beukes NJ
863 (2004) Dating the rise of atmospheric oxygen. *Nature,* **427**, 117-120.
864 Berner RA (1970) Sedimentary pyrite formation. *Am J Sci,* **268**, 1-23.
865 Blake RE, Surkov AV, Böttcher ME, Ferdelman TG, Jørgensen BB (2006) Oxygen isotope
866 composition of dissolved sulfate in deep-sea sediments: eastern equatorial Pacific Ocean.
867 In: *Proceedings of the Ocean Drilling Program, Scientific Results* (eds Jørgensen BB,
868 D'hondt SL, Miller DJ), pp. 1-23.
869 Boesen C, Postma D (1988) Pyrite formation in anoxic environments of the Baltic. *Am J Sci,*
870 **288**, 575-603.
871 Bolliger C, Schroth MH, Bernasconi SM, Kleikemper J, Zeyer J (2001) Sulfur isotope
872 fractionation during microbial sulfate reduction by toluene-degrading bacteria.
873 *Geochimica et Cosmochimica Acta,* **65**, 3289-3298.
874 Böttcher ME, Oelschläger B, Höpner T, Brumsack H-J, Rullkötter J (1998) Sulfate reduction
875 related to the early diagenetic degradation of organic matter and "black spot" formation in
876 tidal sandflats of the German Wadden Sea (southern North Sea): stable isotope (13C,
877 34S, 18O) and other geochemical results. *Organic Geochemistry,* **29**, 1517-1530.
878 Böttcher ME, Thamdrup B, Vennemann TW (2001) Oxygen and sulfur isotope fractionation
879 during anaerobic bacterial disproportionation of elemental sulfur. *Geochimica et*
880 *Cosmochimica Acta,* **65**, 1601-1609.
881 Bottrell SH, Newton RJ (2006) Reconstruction of changes in global sulfur cycling from marine
882 sulfate isotopes. *Earth-Science Reviews,* **75**, 59-83.
883 Brabec MY, Lyons TW, Mandernack KW (2012) Oxygen and Sulfur Isotope Fractionation
884 during Sulfide Oxidation by Anoxygenic Phototrophic Bacteria. *Geochimica et*
885 *Cosmochimica Acta,* **83**, 234-251.
886 Bradley AS, Leavitt WD, Johnston DT (2011) Revisiting the dissimilatory sulfate reduction
887 pathway. *Geobiology,* **9**, 446-457.
888 Brocks JJ, Love GD, Summons RE, Knoll AH, Logan GA, Bowden SA (2005) Biomarker
889 evidence for green and purple sulphur bacteria in a stratified Palaeoproterozoic sea.
890 *Nature,* **437**, 866-870.

Brocks JJ, Schaeffer P (2008) Okenane, a biomarker for purple sulfur bacteria (Chromatiaceae), and other new carotenoid derivatives from the 1640 Ma Barney Creek Formation. *Geochimica et Cosmochimica Acta,* **72**, 1396-1414.

Brüchert V, Knoblauch C, Jørgensen BB (2001) Controls on stable sulfur isotope fractionation during bacterial sulfate reduction in Arctic sediments. *Geochimica et Cosmochimica Acta,* **65**, 763-776.

Brunner B, Bernasconi SM (2005) A revised isotope fractionation model for dissimilatory sulfate reduction in sulfate reducing bacteria. *Geochimica et Cosmochimica Acta,* **69**, 4759-4771.

Brunner B, Bernasconi SM, Kleikemper J, Schroth MH (2005) A model for oxygen and sulfur isotope fractionation in sulfate during bacterial sulfate reduction processes. *Geochimica et Cosmochimica Acta,* **69**, 4773-4785.

Brunner B, Einsiedl F, Arnold GL, Müller I, Templer S, Bernasconi SM (2012) The reversibility of dissimilatory sulphate reduction and the cell-internal multi-step reduction of sulphite to sulphide: insights from the oxygen isotope composition of sulphate. *Isotopes in environmental and health studies,* **48**, 33-54.

Calmels D, Gaillardet J, Brenot A, France-Lanord C (2007) Sustained sulfide oxidation by physical erosion processes in the Mackenzie River basin: Climatic perspectives. *Geology,* **35**, 1003-1006.

Canfield DE (1998) A new model for Proterozoic ocean chemistry. *Nature,* **396**, 450-453.

Canfield DE (2001) Biogeochemistry of Sulfur Isotopes. In: *Stable Isotope Geochemistry* (eds Valley JW, Cole DR). Mineralogical Society of America, Washington DC, pp. 607-636.

Canfield DE, Farquhar J (2009) Animal evolution, bioturbation, and the sulfate concentration of the oceans. *Proceedings of the National Academy of Sciences,* **106**, 8123-8127.

Canfield DE, Farquhar J, Zerkle AL (2010) High isotope fractionations during sulfate reduction in a low-sulfate euxinic ocean analog. *Geology,* **38**, 415-418.

Canfield DE, Raiswell R, Westrich JT, Reaves CM, Berner RA (1986) The use of chromium reduction in the analysis of reduced inorganic sulfur in sediments and shales. *Chemical Geology,* **54**, 149-155.

Canfield DE, Teske A (1996) Late Proterozoic rise in atmospheric oxygen concentration inferred from phylogenetic and sulphur-isotope studies. *Nature* **382**, 127-132.

Canfield DE, Thamdrup B (1994) The Production of ^{34}S-Depleted Sulfide During Baterial Disproportionation of Elemental Sulfur. *Science,* **266**, 1973-1975.

Chambers LA, Trudinger PA, Smith JW, Burns MS (1975) Fractionation of sulfur isotopes by continuous cultures of Desulfovibrio desulfuricans. *Canadian Journal of Microbiology,* **21**, 1602-1607.

Chanton J, Martens C (1985) The effects of heat and stannous chloride addition on the active distillation of acid volatile sulfide from pyrite-rich marine sediment samples. *Biogeochemistry,* **1**, 375-382-382.

Chiba H, Sakai H (1985) Oxygen isotope exchange rate between dissolved sulfate and water at hydrothermal temperatures. *Geochimica et Cosmochimica Acta,* **49**, 993-1000.

Chu X, Ohmoto H, Cole DR (2004) Kinetics of sulfur isotope exchange between aqueous sulfide and thiosulfate involving intra-and intermolecular reactions at hydrothermal conditions. *Chemical Geology,* **211**, 217-235.

Church BN (2002) Geoscience Map 2002-5: Geology of the Penticton Tertiary Outlier, British Columbia (NTS 082E/5).

937 Claypool GE, Holser WT, Kaplan IR, Sakai H, Zak I (1980) The age curves of sulfur and oxygen
938 isotopes in marine sulfate and their mutual interpretation. *Chemical Geology,* **28**, 199-
939 260.
940 Cline JD (1969) Spectrophotometric Determination of Hydrogen Sulfide in Natural Waters.
941 *Limnology and Oceanography,* **14**, 454-458.
942 Coolen MJL, Overmann J (1998) Analysis of Subfossil Molecular Remains of Purple Sulfur
943 Bacteria in a Lake Sediment. *Applied and Environmental Microbiology,* **64**, 4513-4521.
944 Cornwell JC, Morse JW (1987) The characterization of iron sulfide minerals in anoxic marine
945 sediments. *Marine Chemistry,* **22**, 193-206.
946 Criss RE, Fleck RJ, Taylor HP (1991) Tertiary Meteoric Hydrothermal Systems and their
947 Relation to Ore Deposition, Northwestern United States and Southern British Columbia.
948 *Journal of Geophysical Research,* **96**, 13,335-313,356.
949 Crowe SA, Paris G, Katsev S, Jones C, Kim S-T, Zerkle AL, Nomosatryo S, Fowle DA, Adkins
950 JF, Sessions AL, Farquhar J, Canfield DE (2014) Sulfate was a trace constituent of
951 Archean seawater. *Science,* **346**, 735-739.
952 Deevey ES, Nakai N, Stuiver M (1963) Fractionation of Sulfur and Carbon Isotopes in a
953 Meromictic Lake. *Science,* **139**, 407-407.
954 Detmers J, Bruchert V, Habicht KS, Kuever J (2001) Diversity of Sulfur Isotope Fractionations
955 by Sulfate-Reducing Prokaryotes. *Appl. Environ. Microbiol.,* **67**, 888-894.
956 Dickman M (1985) Seasonal succession and microlamina formation in a meromictic lake
957 displaying varved sediments. *Sedimentology,* **32**, 109-118.
958 Dickman MD, Thode HG (1990) Sulfur bacteria and sulfur isotope fractionation in a meromictic
959 lake near Toronto, Canada. In: *Facets of modern biogeochemistry* (eds Ihebhot V, Kempe
960 S, Michaelis W, Spitzg A). Springer-Verlag, pp. 225-241.
961 Farquhar J, Bao H, Thiemens M (2000) Atmospheric Influence of Earth's Earliest Sulfur Cycle.
962 *Science,* **289**, 756-758.
963 Farquhar J, Johnston DT, Wing BA (2007) Implications of conservation of mass effects on mass-
964 dependent isotope fractionations: Influence of network structure on sulfur isotope phase
965 space of dissimilatory sulfate reduction. *Geochimica et Cosmochimica Acta,* **71**, 5862-
966 5875.
967 Farquhar J, Johnston DT, Wing BA, Habicht KS, Canfield DE, Airieau S, Thiemens MH (2003)
968 Multiple sulphur isotopic interpretations of biosynthetic pathways: implications for
969 biological signatures in the sulphur isotope record. *Geobiology,* **1**, 27-36.
970 Fike DA, Grotzinger JP, Pratt LM, Summons RE (2006) Oxidation of the Ediacaran Ocean.
971 *Nature,* **444**, 744-747.
972 Fisher MM, Brenner M, Reddy KR (1992) A simple, inexpensive piston corer for collecting
973 undisturbed sediment/water interface profiles. *Journal of Paleolimnology,* **7**, 157-161-
974 161.
975 Fritz P, Basharmal GM, Drimmie RJ, Ibsen J, Qureshi RM (1989) Oxygen isotope exchange
976 between sulphate and water during bacterial reduction of sulphate. *Chemical Geology,*
977 **79**, 99-105.
978 Fry B (1986) Sources of Carbon and Sulfur Nutrition for Consumers in Three Meromictic Lakes
979 of New York State. *Limnology and Oceanography,* **31**, 79-88.
980 Fry B, Cox J, Gest H, Hayes JM (1986) Discrimination between ^{34}S and ^{32}S during Bacterial
981 Metabolism of Inorganic Sulfur Compounds. *Journal of Bacteriology,* **165**, 328-330.

982 Fry B, Gest H, Hayes JM (1984) Isotope effects associated with the anaerobic oxidation of
983 sulfide by the purple photosynthetic bacterium, Chromatium vinosum. *FEMS*
984 *Microbiology Letters,* **22**, 283-287.
985 Fry B, Gest H, Hayes JM (1988a) $^{34}S/^{32}S$ fractionation in sulfur cycles catalyzed by anaerobic
986 bacteria. *Appl. Environ. Microbiol.,* **54**, 250-256.
987 Fry B, Jannasch HW, Molyneaux SJ, Wirsen CO, Muramoto JA, King S (1991) Stable isotope
988 studies of the carbon, nitrogen and sulfur cycles in the Black Sea and Cariaco Trench.
989 *Deep Sea Research,* **38**, S1003-S1019.
990 Fry B, Ruf W, Gest H, Hayes JM (1988b) Sulfur Isotope Effects Associated with Oxidation of
991 Sulfide by O_2 in Aqueous Solution. *Chemical Geology,* **73**, 205-210.
992 Gibson JJ, Edwards TWD, Birks SJ, St Amour NA, Buhay WM, Mceachern P, Wolfe BB, Peters
993 DL (2005) Progress in isotope tracer hydrology in Canada. *Hydrological Processes,* **19**,
994 303-327.
995 Gibson JJ, Prepas EE, Mceachern P (2002) Quantitative comparison of lake throughflow,
996 residency, and catchment runoff using stable isotopes: modelling and results from a
997 regional survey of Boreal lakes. *Journal of Hydrology,* **262**, 128-144.
998 Habicht KS, Canfield DE, Rethmeier J (1998) Sulfur isotope fractionation during bacterial
999 reduction and disproportionation of thiosulfate and sulfite. *Geochimica et Cosmochimica*
1000 *Acta,* **62**, 2585-2595.
1001 Habicht KS, Gade M, Thamdrup B, Berg P, Canfield DE (2002) Calibration of Sulfate Levels in
1002 the Archean Ocean. *Science,* **298**, 2372-2374.
1003 Hamilton T, Bovee R, Thiel V, Sattin S, Mohr W, Schaperdoth I, Vogl K, Gilhooly W, Lyons T,
1004 Tomsho L (2014) Coupled reductive and oxidative sulfur cycling in the phototrophic
1005 plate of a meromictic lake. *Geobiology,* **12**, 451-468.
1006 Harrison AG, Thode HG (1958) Mechanisms of the bacterial reduction of sulphate from isotope
1007 fractionation studies. *Transactions of the Faraday Society,* **54**, 85-92.
1008 Heinrichs M, Wilson S, Walker I, Smol J, Mathewes R, Hall K (1997) Midge-and diatom-based
1009 palaeosalinity reconstructions for Mahoney Lake, Okanagan Valley, British Columbia,
1010 Canada. *International Journal of Salt Lake Research,* **6**, 249-267.
1011 Hoering TC, Kennedy JW (1957) The Exchange of Oxygen between Sulfuric Acid and Water1.
1012 *Journal of the American Chemical Society,* **79**, 56-60.
1013 Holser WT, Kaplan IR, Sakai H, Zak I (1979) Isotope geochemistry of oxygen in the
1014 sedimentary sulfate cycle. *Chemical Geology,* **25**, 1-17.
1015 Hurtgen MT, Arthur MA, Halverson GP (2005) Neoproterozoic sulfur isotopes, the evolution of
1016 microbial sulfur species, and the burial efficiency of sulfide as sedimentary pyrite.
1017 *Geology,* **33**, 41-44.
1018 Johnston DT, Farquhar J, Canfield DE (2007) Sulfur isotope insights into microbial sulfate
1019 reduction: When microbes meet models. *Geochimica et Cosmochimica Acta,* **71**, 3929-
1020 3947.
1021 Johnston DT, Wing BA, Farquhar J, Kaufman AJ, Strauss H, Lyons TW, Kah LC, Canfield DE
1022 (2005) Active Microbial Sulfur Disproportionation in the Mesoproterozoic. *Science,* **310**,
1023 1477-1479.
1024 Johnston DT, Wolfe-Simon F, Pearson A, Knoll AH (2009) Anoxygenic photosynthesis
1025 modulated Proterozoic oxygen and sustained Earth's middle age. *Proceedings of the*
1026 *National Academy of Sciences,* **106**, 16925-16929.

1027 Kaplan IR, Rittenberg SC (1964a) Microbiological Fractionation of Sulphur Isotopes. *Journal of*
1028 *General Microbiology,* **34**, 195-212.
1029 Kaplan IR, Rittenberg SC (1964b) Microbiological Fractionation of Sulphur Isotopes.
1030 *Microbiology,* **34**, 195-212.
1031 Kemp ALW, Thode HG (1968) The mechanism of the bacterial reduction of sulphate and of
1032 sulphite from isotope fractionation studies. *Geochimica et Cosmochimica Acta,* **32**, 71-
1033 91.
1034 Klepac-Ceraj V, Hayes CA, Gilhooly WP, Lyons TW, Kolter R, Pearson A (2012) Microbial
1035 diversity under extreme euxinia: Mahoney Lake, Canada. *Geobiology,* **10**, 223-235.
1036 Knöller K, Vogt C, Richnow H-H, Weise S (2006) Sulfur and Oxygen Isotope Fractionation
1037 during Benzene, Toluene, Ethyl Benzene, and Xylene Degradation by Sulfate-Reducing
1038 Bacteria. *Environmental Science and Technology,* **40**, 3879-3885.
1039 Leavitt WD, Cummins R, Schmidt ML, Sim MS, Ono S, Bradley AS, Johnston DT (2014)
1040 Multiple sulfur isotope signatures of sulfite and thiosulfate reduction by the model
1041 dissimilatory sulfate-reducer, Desulfovibrio alaskensis str. G20. *Frontiers in*
1042 *microbiology,* **5**.
1043 Leavitt WD, Halevy I, Bradley AS, Johnston DT (2013) Influence of sulfate reduction rates on
1044 the Phanerozoic sulfur isotope record. *Proceedings of the National Academy of Sciences,*
1045 **110**, 11244-11249.
1046 Lewis T (1984) Geothermal energy from Penticton Tertiary outlier, British Columbia: an initial
1047 assessment. *Canadian Journal of Earth Sciences,* **21**, 181-188.
1048 Li X, Gilhooly Iii WP, Zerkle AL, Lyons TW, Farquhar J, Werne JP, Varela R, Scranton MI
1049 (2010) Stable sulfur isotopes in the water column of the Cariaco Basin. *Geochimica et*
1050 *Cosmochimica Acta,* **74**, 6764-6778.
1051 Lloyd RM (1968) Oxygen Isotope Behavior in the Sulfate-Water System. *Journal of*
1052 *Geophysical Research,* **73**, 6099.
1053 Lowe DJ, Green JD, Northcote TG, Hall KJ (1997) Holocene Fluctuations of a Meromictic Lake
1054 in Southern British Columbia. *Quaternary Research,* **48**, 100-113.
1055 Lyons TW (1997) Sulfur isotopic trends and pathways of iron sulfide formation in upper
1056 Holocene sediments of the anoxic Black Sea. *Geochimica et Cosmochimica Acta,* **61**,
1057 3367-3382.
1058 Lyons TW, Berner RA, Anderson RF (1993) Evidence for large pre-industrial perturbations of
1059 the Black Sea chemocline. *Nature,* **365**, 538-540.
1060 Lyons TW, Kah LC, Gellatly AM (2004) The Precambrian sulphur isotope record of evolving
1061 atmospheric oxygen. In: *The Precambrian Earth: Tempos and Events* (eds Eriksson PG,
1062 Alterman W, Nelson DR, Mueller WU, Catuneanu O). Elsevier, Amsterdam, pp. 421-
1063 440.
1064 Lyons TW, Severmann S (2006) A critical look at iron paleoredox proxies: New insights from
1065 modern euxinic marine basins. *Geochimica et Cosmochimica Acta,* **70**, 5698-5722.
1066 Lyons TW, Werne JP, Hollander DJ, Murray RW (2003) Contrasting sulfur geochemistry and
1067 Fe/Al and Mo/Al ratios across the last oxic-to-anoxic transition in the Cariaco Basin,
1068 Venezuela. *Chemical Geology,* **195**, 131-157.
1069 Magaritz M, Taylor HP (1986) Oxygen 18/Oxygen 16 and D/H Studies of Plutonic Granitic and
1070 Metamorphic Rocks Across the Cordilleran Batholiths of Southern British Columbia.
1071 *Journal of Geophysical Research,* **91**, 2193-2217.

1072 Mandernack KW, Krouse HR, Skei JM (2003) A stable sulfur and oxygen isotopic investigation
1073 of sulfur cycling in an anoxic marine basin, Framvaren Fjord, Norway. *Chemical*
1074 *Geology,* **195**, 181-200.
1075 Mariotti A, Germon J, Hubert P, Kaiser P, Letolle R, Tardieux A, Tardieux P (1981)
1076 Experimental determination of nitrogen kinetic isotope fractionation: Some principles;
1077 illustration for the denitrification and nitrification processes. *Plant and Soil,* **62**, 413-430-
1078 430.
1079 Meyer K, Macalady J, Fulton J, Kump L, Schaperdoth I, Freeman K (2011) Carotenoid
1080 biomarkers as an imperfect reflection of the anoxygenic phototrophic community in
1081 meromictic Fayetteville Green Lake. *Geobiology,* **9**, 321-329.
1082 Michel FA, Allen DM, Grant MB (2002) Hydrogeochemistry and geothermal characteristics of
1083 the White Lake basin, South-central British Columbia, Canada. *Geothermics,* **31**, 169-
1084 194.
1085 Mizutani Y (1972) Isotopic composition and underground temperature of the Otake geothermal
1086 water Kyushu, Japan. *Geochemical Journal,* **6**, 67-73.
1087 Mizutani Y, Rafter TA (1969) Oxygen Isotopic Composition of Sulphates - Part 4. *New Zealand*
1088 *Journal of Science,* **12**, 60-68.
1089 Mizutani Y, Rafter TA (1973) Isotopic behaviour of sulfate oxygen in the bacterial reduction of
1090 sulfate. *Gechemical Journal,* **6**, 183-191.
1091 Neretin LN, Bˆttcher ME, Grinenko VA (2003) Sulfur isotope geochemistry of the Black Sea
1092 water column. *Chemical Geology,* **200**, 59-69.
1093 Northcote T, Hall K (2010) Salinity regulation of zooplanktonic abundance and vertical
1094 distribution in two saline meromictic lakes in south central British Columbia.
1095 *Hydrobiologia,* **638**, 121-136.
1096 Northcote TG, Hall KJ (1983) Limnological contrasts and anomalies in two adjacent saline
1097 lakes. *Hydrobiologia,* **105**, 179-194.
1098 Northcote TG, Hall KJ (1990) Vernal microstratification patterns in a meromictic saline lake:
1099 their causes and biological significance. *Hydrobiologia,* **197**, 105-114-114.
1100 Northcote TG, Hall KJ (2000) Short-term (decadal, annual, seasonal) changes in the limnology
1101 of a saline uni-/bimeromictic lake: causes and consequences. *Verhandlugen*
1102 *Internationale Vereinigen für theoretische und angewandte Limnologie* **27**, 2652-2659.
1103 Northcote TG, Halsey TG (1969) Seasonal changes in the limnology of some meromictic lakes
1104 in southern British Columbia. *Journal Fisheries Research Board of Canada,* **26**, 1763-
1105 1787.
1106 Ohmoto H, Lasaga AC (1982) Kinetics of reactions between aqueous sulfates and sulfides in
1107 hydrothermal systems. *Geochimica et Cosmochimica Acta,* **46**, 1727-1745.
1108 Overmann J (1997) Mahoney Lake: A case study of the ecological significance of phototrophic
1109 sulfur bacteria. In: *Advances in Microbial Ecology* (ed Jones JG). Plenum Press, New
1110 York.
1111 Overmann J, Beatty JT, Hall KJ, Pfennig N, Northcote TG (1991) Characterization of a dense,
1112 purple sulfur bacterial layer in a meromictic salt lake. *Limnology and Oceanography,* **36**,
1113 846-859.
1114 Overmann J, Beatty JT, Krouse HR, Hall KJ (1996) The sulfur cycle in the chemocline of a
1115 meromictic salt lake. *Limnology and Oceanography,* **4**, 147-156.
1116 Overmann J, Pfennig N (1992) Bouyancy regulation and aggregate formation in Amoebobacter
1117 purpureus from Mahoney Lake. *FEMS Microbiology Letters,* **101**, 67-79.

1118 Overmann J, Sandmann G, Hall KJ, Northcote TG (1993) Fossil carotenoids and paleolimnology
1119 of meromictic Mahoney Lake, British Columbia, Canada. *Aquatic Sciences - Research*
1120 *Across Boundaries,* **55**, 31-39.
1121 Overmann J, Thomas Beatty J, Hall KJ (1994) Photosynthetic activity and population dynamics
1122 of Amoebobacter purpureus in a meromictic saline lake. *FEMS Microbiology Ecology,*
1123 **15**, 309-319.
1124 Raiswell R, Buckley F, Berner RA, Anderson TF (1988) Degree of pyritization of iron as a
1125 paleoenvironmental indicator of bottom-water oxygenation. *Journal of Sedimentary*
1126 *Research,* **58**, 812-819.
1127 Raiswell R, Canfield DE, Berner RA (1994) A comparison of iron extraction methods for the
1128 determination of degree of pyritisation and the recognition of iron-limited pyrite
1129 formation. *Chemical Geology,* **111**, 101-110.
1130 Rees CE (1973) A steady-state model for sulphur isotope fractionation in bacterial reduction
1131 processes. *Geochimica et Cosmochimica Acta,* **37**, 1141-1162.
1132 Rees CE (1978) The sulphur isotopic composition of ocean water sulphate. *Geochimica et*
1133 *Cosmochimica Acta,* **42**, 377-381.
1134 Reinhard CT, Planavsky NJ, Robbins LJ, Partin CA, Gill BC, Lalonde SV, Bekker A, Konhauser
1135 KO, Lyons TW (2013) Proterozoic ocean redox and biogeochemical stasis. *Proceedings*
1136 *of the National Academy of Sciences,* **110**, 5357-5362.
1137 Riedinger N, Brunner B, Formolo MJ, Solomon E, Kasten S, Strasser M, Ferdelman TG (2010)
1138 Oxidative sulfur cycling in the deep biosphere of the Nankai Trough, Japan. *Geology,* **38**,
1139 851-854.
1140 Rudnicki MD, Elderfield H, Spiro B (2001) Fractionation of sulfur isotopes during bacterial
1141 sulfate reduction in deep ocean sediments at elevated temperatures. *Geochimica et*
1142 *Cosmochimica Acta,* **65**, 777-789.
1143 Sheu D-D, Shakur A, Pigott JD, Wiesenburg DA, Brooks JM, Krouse HR (1988) Sulfur and
1144 oxygen isotopic compositions of dissolved sulfate in the Orca Basin: Implications for
1145 origin of the high-salinity brine and oxidation of sulfides at the brine-seawater interface.
1146 *Marine Geology,* **78**, 303-310.
1147 Sim MS, Bosak T, Ono S (2011) Large Sulfur Isotope Fractionation Does Not Require
1148 Disproportionation. *Science,* **333**, 74-77.
1149 Sørensen KB, Canfield DE (2004) Annual fluctuations in sulfur isotope fractionation in the water
1150 column of a euxinic marine basin. *Geochimica et Cosmochimica Acta,* **68**, 503-515.
1151 Stookey LL (1970) Ferrozine---a new spectrophotometric reagent for iron. *Analytical Chemistry,*
1152 **42**, 779-781.
1153 Sweeney RE, Kaplan IR (1980) Stable isotope composition of dissolved sulfate and hydrogen
1154 sulfide in the Black Sea. *Marine Chemistry,* **9**, 145-152.
1155 Taylor BE, Wheeler MC (1984) Isotope composition of sulphate in acid mine drainage as
1156 measure of bacterial oxidation. *Nature,* **308**, 538-541.
1157 Thamdrup B, Finster K, Hansen JW, Bak F (1993) Bacterial Disproportionation of Elemental
1158 Sulfur Coupled to Chemical Reduction of Iron or Manganese. *Applied and*
1159 *Environmental Microbiology,* **59**, 101-108.
1160 Turchyn AV, Brüchert V, Lyons TW, Engel GS, Balci N, Schrag DP, Brunner B (2010) Kinetic
1161 oxygen isotope effects during dissimilatory sulfate reduction: a combined theoretical and
1162 experimental approach. *Geochimica et Cosmochimica Acta,* **74**, 2011-2024.

1163 Turchyn AV, Schrag DP (2006) Cenozoic evolution of the sulfur cycle: Insight from oxygen
1164 isotopes in marine sulfate. *Earth and Planetary Science Letters,* **241**, 763-779.
1165 Turchyn AV, Schrag DP, Coccioni R, Montanari A (2009) Stable isotope analysis of the
1166 Cretaceous sulfur cycle. *Earth and Planetary Science Letters,* **285**, 115-123.
1167 Van Everdingen RO, Krouse HR (1985) Isotope composition of sulphates generated by bacterial
1168 and abiological oxidation. *Nature,* **315**, 395-396.
1169 Ward PRB, Cousins EA, Hall KJ, Northcote TG, Murphy TP (1989) Mixing by Wind and
1170 Penetrative Convection in Small Lakes. In: *International Association for Hydraulic*
1171 *Research, 23rd. Congress*, Ottawa, Canada, pp. D-331-D-338.
1172 Ward PRB, Hall KJ, Northcote TG, Cheung W, Murphy T (1990) Autumnal mixing in Mahoney
1173 Lake, British Columbia. *Hydrobiologia,* **197**, 129-138-138.
1174 Wehrmann LM, Templer SP, Brunner B, Bernasconi SM, Maignien L, Ferdelman TG (2011)
1175 The imprint of methane seepage on the geochemical record and early diagenetic
1176 processes in cold-water coral mounds on Pen Duick Escarpment, Gulf of Cadiz. *Marine*
1177 *Geology,* **282**, 118-137.
1178 West AG, Patrickson SJ, Ehleringer JR (2006) Water extraction times for plant and soil materials
1179 used in stable isotope analysis. *Rapid Communications in Mass Spectrometry,* **20**, 1317-
1180 1321.
1181 Wortmann UG, Bernasconi SM, Bottcher ME (2001) Hypersulfidic deep biosphere indicates
1182 extreme sulfur isotope fractionation during single-step microbial sulfate reduction.
1183 *Geology,* **29**, 647-650.
1184 Wortmann UG, Chernyavsky B, Bernasconi SM, Brunner B, Bˆttcher ME, Swart PK (2007)
1185 Oxygen isotope biogeochemistry of pore water sulfate in the deep biosphere: Dominance
1186 of isotope exchange reactions with ambient water during microbial sulfate reduction
1187 (ODP Site 1130). *Geochimica et Cosmochimica Acta,* **71**, 4221-4232.
1188 Zak I, Saki H, Kaplan IR (1980) Factors Controlling the $^{18}O/^{16}O$ and $^{34}S/^{32}S$ Isotope Ratios of
1189 Ocean Sulfates, Evaporites and Interstitial Sulfates from Modern Deep Sea Sediments.
1190 In: *Isotope Marine Chemistry* (eds Goldberg ED, Horibe Y, Saruhashi K). Geochemistry
1191 Research Association, Tokyo, pp. 339-373.
1192 Zeebe RE (2010) A new value for the stable oxygen isotope fractionation between dissolved
1193 sulfate ion and water. *Geochimica et Cosmochimica Acta,* **74**, 818-828.
1194 Zerkle AL, Farquhar J, Johnston DT, Cox RP, Canfield DE (2009) Fractionation of multiple
1195 sulfur isotopes during phototrophic oxidation of sulfide and elemental sulfur by a green
1196 sulfur bacterium. *Geochimica et Cosmochimica Acta,* **73**, 291-306.
1197 Zerkle AL, Kamyshny Jr A, Kump LR, Farquhar J, Oduro H, Arthur MA (2010) Sulfur cycling
1198 in a stratified euxinic lake with moderately high sulfate: Constraints from quadruple S
1199 isotopes. *Geochimica et Cosmochimica Acta,* **74**, 4953-4970.
1200 Zhang J-Z, Millero FJ (1994) Kinetics of Oxidation of Hydrogen Sulfide in Natural Waters. In:
1201 *Environmental Geochemistry of Sulfide Oxidation* (eds Alpers CN, Blowes DW).
1202 American Chemical Society, Washingon DC, pp. 393-409.
1203 Zopfi J, Ferdelman TG, Jörgensen BB, Teske A, Thamdrup B (2001) Influence of water column
1204 dynamics on sulfide oxidation and other major biogeochemical processes in the
1205 chemocline of Mariager Fjord (Denmark). *Marine Chemistry,* **74**, 29-51.
1206

1207

Figure 1. Mahoney Lake and Green Lake are located within the White Lake Basin, British Columbia (modified after Northcote and Hall, 1983; Michel et al, 2002). Cores 2 and 3 were collected from the center of Mahoney Lake and Core 9 was taken from the oxic margin. Surface water $\delta^{34}S_{SO4}$, $\delta^{18}O_{SO4}$, and sulfate concentrations are shown for Mahoney Lake, Green Lake, Sleeping Lake, and the upland pond (ML pond), as well as the $\delta^{34}S$ of chromium reducible sulfur extracted from a greenstone sample collected from the eastern side of the catchment. Bedrock geology transitions from meta-volcanics west of the fault-line to cherts and greenstones east of the fault. Geologic descriptions and interpretations are from Church (2002) and Northcote and Hall (1983).

Figure 2. Oxygen and hydrogen isotope data for meteoric water and surface waters in the White Lake Basin. Results from the current study include samples from the Mahoney Lake mixolimnion (ML 08 oxic) and monimolimnion (ML 08 anoxic), the upland pond (ML pond 08), and Sleeping Lake (SL 08). All remaining water data are from Michel et al., (2002). The Local Meteoric Water Line (LMWL) is shown for Penticton precipitation data (squares) in comparison to the Global Meteoric Water Line (GMWL; $\delta D = 8\delta^{18}O + 10$). Data for deep wells (open diamonds; 76 to 549 m deep), shallow wells drilled in overburden (filled diamonds), springs (triangles), and surface waters (circles) all plot along a local evaporation line (LEL) with a slope of 4.7 ($R^2 = 0.99$). The inset shows LEL relative to the isotopic composition of Vienna Standard Mean Oceanwater (VSMOW) and Okanagan granitic batholiths (Magaritz and Taylor, 1986).

Figure 3. Water column profiles of temperature, specific conductivity (SpC), pH, dissolved oxygen (DO), dissolved sulfide (H_2S), light intensity, and turbidity for (A) Mahoney and Green Lake in September 2006, and (B) Mahoney Lake in July 2008. Extinction coefficients (k) were calculated for light attenuation above ($k = 0.400$) and below the chemocline ($k = 3.347$) in Mahoney Lake, July 2008.

Figure 4. Mahoney Lake water column profiles of chloride and sulfate concentrations, SO_4/Cl (molar), $\delta^{34}S_{H2S}$, $\delta^{34}S_{SO4}$, and $\delta^{18}O_{SO4}$ for samples collected in September 2006 (filled symbols) and July 2008 (open symbols). Vertical shaded regions are the mean plus standard deviations for concentrations ($[Cl] = 57.7 \pm 1.7$ mM; $[SO_4] = 341 \pm 20.1$ mM) or molar ratios ($SO_4/Cl = 5.9 \pm 0.2$) within the upper 5 m of the (oxygenated) water column.

Figure 5. Mahoney Lake (A) solid phase sulfur concentrations, DOS, and (B) solid phase and pore water isotope data for sediments collected below the chemocline (Core 2 and 3) and below oxygenated bottom water (Core 9). Vertical shaded regions (B) indicate the average stable isotope value (± standard deviation) of water column sulfate and sulfide.

Figure 6. Mahoney Lake sulfur isotope fractionation ($\Delta^{34}S_{SO4\text{-}H2S} = \delta^{34}S_{SO4} - \delta^{34}S_{H2S}$) within the water column (round symbols) and averaged pore water values from Cores 2 and 3 (open diamonds) and Core 9 (filled diamonds) plotted against depth. Error bars represent standard

deviation for fractionations. Cores 2 and 3 were collected below the chemocline and Core 9 was collected below oxygenated bottom waters.

Figure 7. Sulfate sulfur and oxygen isotope cross-plots of Mahoney Lake water column sulfate collected in September 2006 (filled symbols) and July 2008 (open symbols). The data are bounded by model arrays (A) that define the expected trajectories of rapid sulfate reduction, Trend A, and slow rates of sulfate reduction, Trend B, based on the initial isotopic compositions for Mahoney Lake sulfate ($\delta^{34}S_{SO4}$ = 21.5‰ and $\delta^{18}O_{SO4}$ = 16.5‰; filled square) and water ($\delta^{18}O_{water}$ = -0.3‰). The data collected in the fall (B) have a higher slope than the those collected in the summer (C).

Figure 8. Mixing plots (δ vs. 1/concentration) of sulfate (A) sulfur isotope and (B) oxygen isotope values relative to sulfate concentration for Mahoney Lake water column (round symbols) and power waters (diamonds) collected from anoxic (open symbols) or oxic (closed symbols) bottom waters.

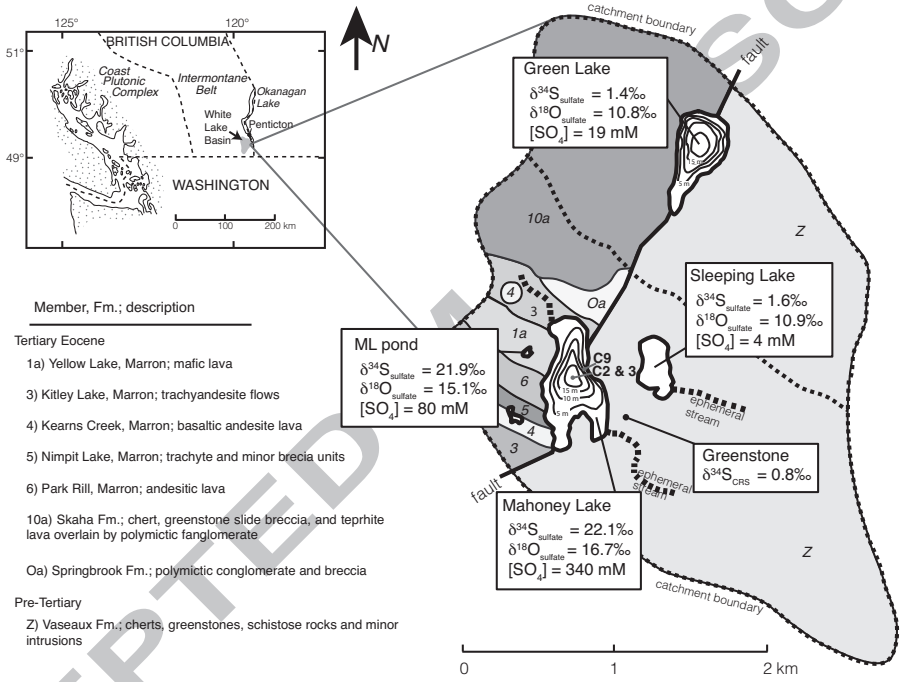

1274
1275

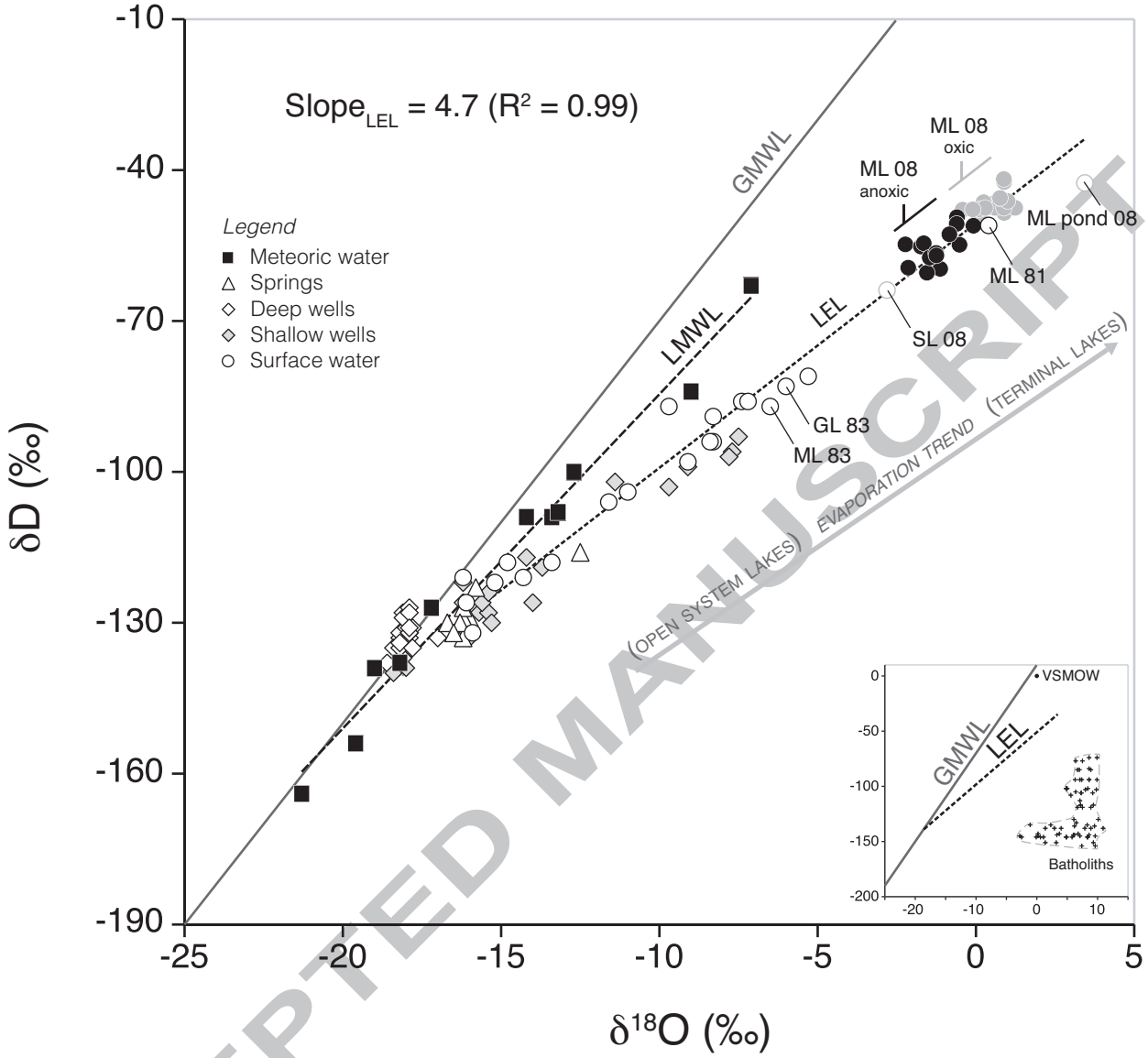

1276
1277

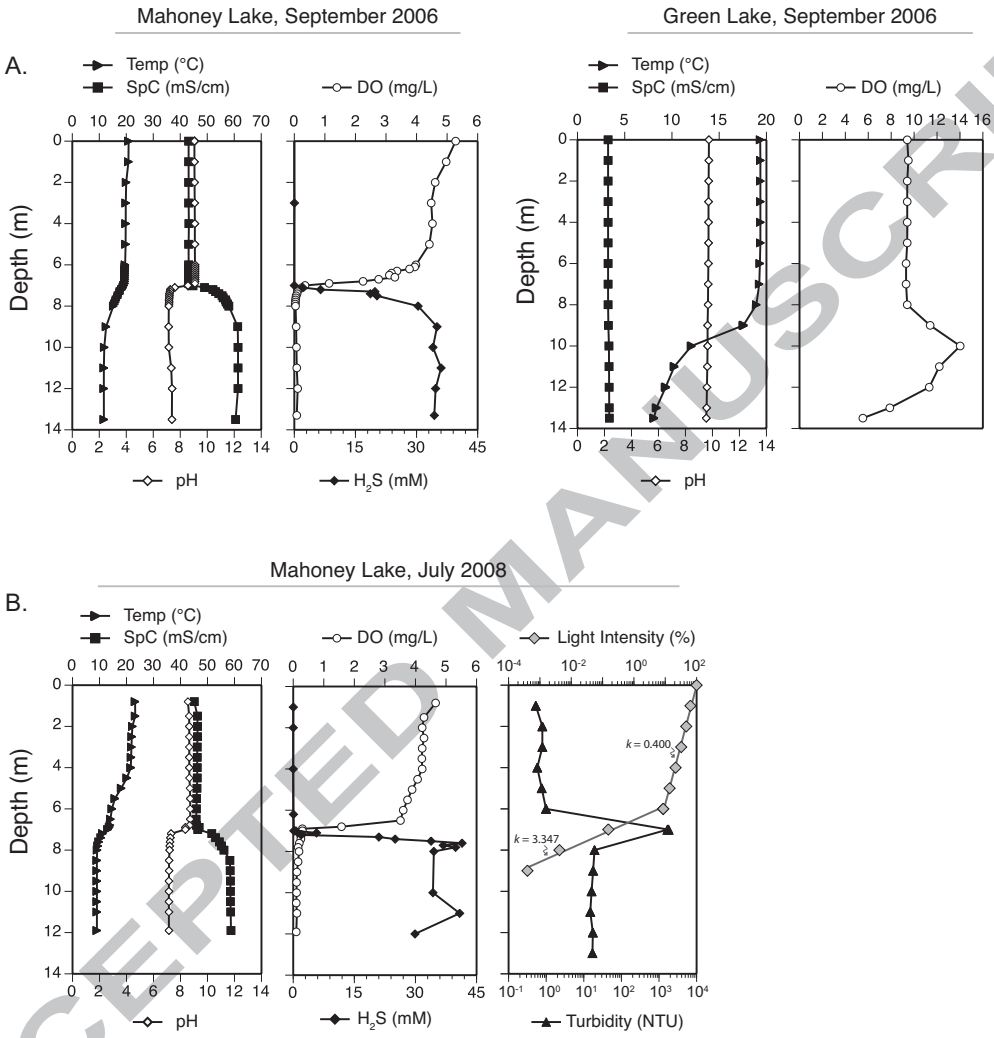

1278
1279

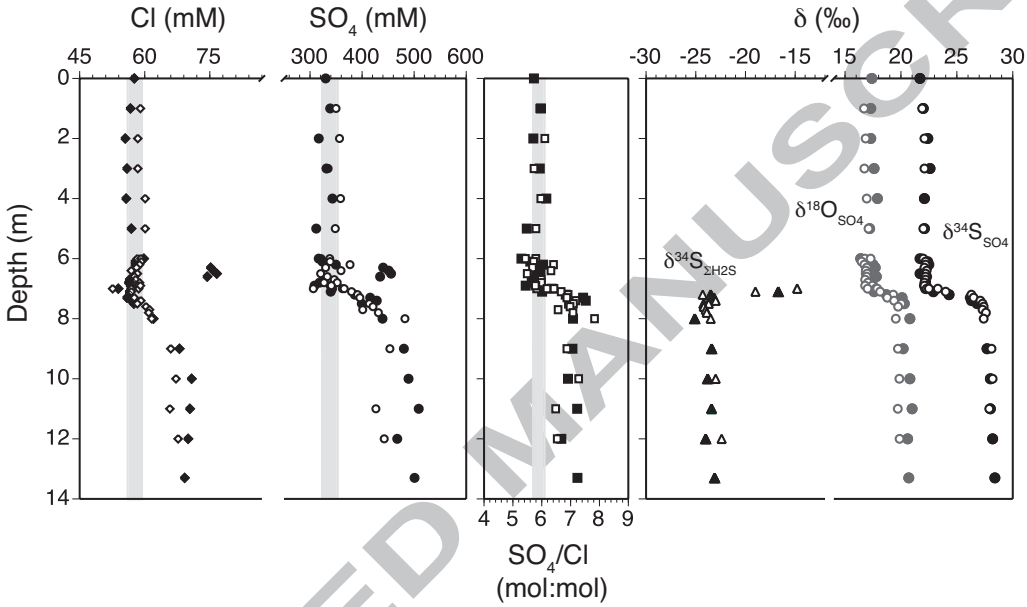

1280
1281

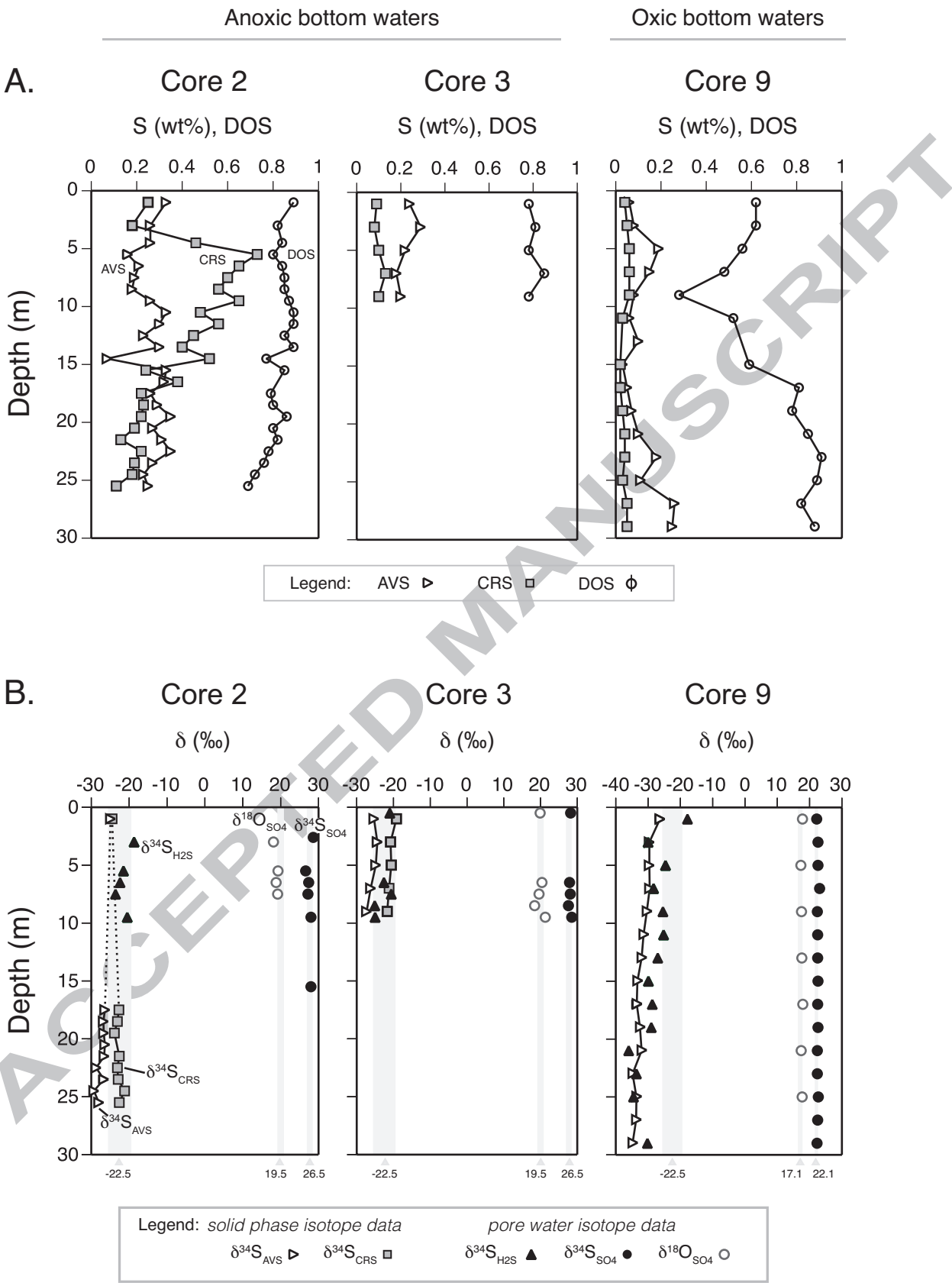

1282
1283

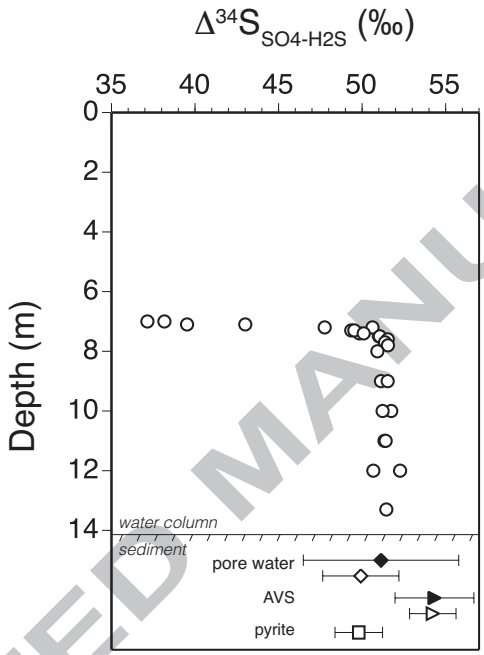

1284
1285

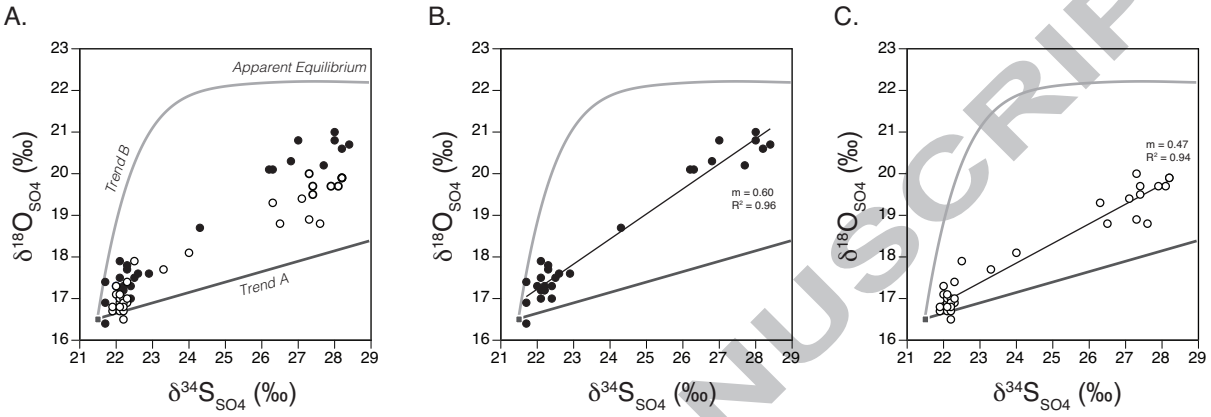

1286
1287

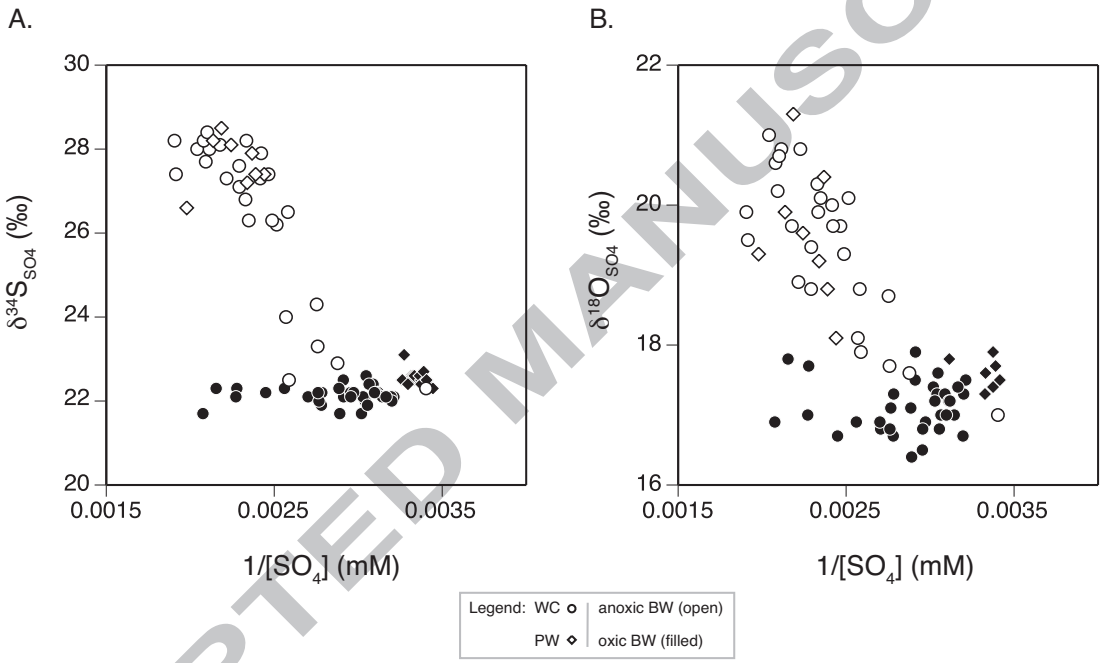

1289 Table 1. Water column concentration and isotope data.

Lake	Depth (m)	ΣH_2S (mM)	SO_4 (mM)	Cl (mM)	$\delta^{18}O_{SO4}$ (‰)	$\delta^{34}S_{SO4}$ (‰)	$\delta^{34}S_{H2S}$ (‰)	$\Delta^{34}S_{SO4-H2S}$ (‰)	$\delta^{34}S_{Elem\ S}$ (‰)	$\delta^{18}O_{H2O}$ (‰)	$\delta^{2}H_{H2O}$ (‰)
September 2006											
Green Lake	0	-	24.94	1.4	11.6	5.2	-	-	-	-	-
	1	-	19.90	0.4	10.5	1.2	-	-	-	-	-
	2	-	20.74	0.2	10.2	1.2	-	-	-	-	-
	3	-	18.52	0.4	10.9	1.2	-	-	-	-	-
	4	-	20.04	0.4	10.6	1.0	-	-	-	-	-
	5	-	19.33	0.01	10.7	0.5	-	-	-	-	-
	6	-	20.22	-	10.5	1.1	-	-	-	-	-
	7	-	20.29	2.3	10.5	1.1	-	-	-	-	-
	9	-	20.09	1.3	11.2	1.1	-	-	-	-	-
	10	-	20.90	0.7	11.0	1.2	-	-	-	-	-
	11	-	21.30	0.7	-	1.0	-	-	-	-	-
	12	-	20.71	-	10.9	1.1	-	-	-	-	-
	13	-	20.13	-	11.1	0.7	-	-	-	-	-
Mahoney Lake	0	-	331.2	57.6	17.4	21.7	-	-	-	-	-
	1	-	328.8	56.7	17.3	22.0	-	-	-	-	-
	2	-	323.8	55.5	17.3	22.4	-	-	-	-	-
	3	0.029	328.2	55.9	17.6	22.6	-	-	-	-	-
	4	-	343.3	55.7	17.9	22.1	-	-	-	-	-
	5	-	330.2	56.9	17.2	22.1	-	-	-	-	-

Lake	Depth (m)	ΣH_2S (mM)	SO_4 (mM)	Cl (mM)	$\delta^{18}O_{SO4}$ (‰)	$\delta^{34}S_{SO4}$ (‰)	$\delta^{34}S_{H2S}$ (‰)	$\Delta^{34}S_{SO4-H2S}$ (‰)	$\delta^{34}S_{Elem S}$ (‰)	$\delta^{18}O_{H2O}$ (‰)	$\delta^{2}H_{H2O}$ (‰)
	6	-	346.0	59.8	16.4	21.7	-	-	-	-	-
	6.1	-	326.3	57.8	17.0	22.4	-	-	-	-	-
	6.2	-	343.5	57.8	17.5	22.5	-	-	-	-	-
	6.3	-	439.1	75.2	17.7	22.3	-	-	-	-	-
	6.4	-	440.2	75.8	17.0	22.1	-	-	-	-	-
	6.5	-	481.8	76.6	16.9	21.7	-	-	-	-	-
	6.6	-	464.2	74.4	17.8	22.3	-	-	-	-	-
	6.7	-	321.4	56.5	17.2	22.2	-	-	-	-	-
	6.8	-	320.7	56.3	17.2	22.2	-	-	-	-	-
	6.9	-	311.3	56.7	17.5	22.1	-	-	-	-	-
	7	-	359.3	53.9	17.3	22.2	-	-	-	-	-
	7.1	2.08	347.6	56.5	17.6	22.9	-16.7	39.5	-	-	-
	7.2	6.45	363.3	56.5	18.7	24.3	-23.5	47.8	-22.7	-	-
	7.3	19.79	397.7	55.9	20.1	26.2	-23.2	49.3	-	-	-
	7.4	18.68	425.8	56.9	20.1	26.3	-23.6	49.8	-	-	-
	7.5	20.29	429.4	57.5	20.3	26.8	-24.2	51.0	-	-	-
	8	30.38	448.9	62.0	20.8	27.0	-25.1	52.1	-	-	-
	9	35.02	477.9	68.0	20.2	27.7	-23.4	51.1	-	-	-
	10	34.03	473.0	70.8	20.8	28.0	-23.8	51.7	-	-	-
	11	36.02	489.9	70.4	21.0	28.0	-23.4	51.3	-	-	-
	12	34.68	480.8	70.0	20.6	28.2	-24.0	52.3	-	-	-

Lake	Depth (m)	ΣH_2S (mM)	SO_4 (mM)	Cl (mM)	$\delta^{18}O_{SO4}$ (‰)	$\delta^{34}S_{SO4}$ (‰)	$\delta^{34}S_{H2S}$ (‰)	$\Delta^{34}S_{SO4-H2S}$ (‰)	$\delta^{34}S_{Elem S}$ (‰)	$\delta^{18}O_{H2O}$ (‰)	$\delta^{2}H_{H2O}$ (‰)
	13.3	34.36	475.9	69.2	20.7	28.4	-23.1	51.4	-	-	-
July 2008											
Mahoney Lake	1	0.031	359.6	59.0	16.7	21.9	-	-	-	0.89	-48.51
	2	0.012	369.6	58.4	16.8	22.1	-	-	-	0.89	-47.37
	3	-	312.9	58.4	16.7	22.1	-	-	-	1.24	-47.50
	4	0.003	370.2	60.1	16.9	22.1	-	-	-	0.89	-42.37
	5	-	361.5	60.1	17.1	22.0	-	-	-	0.76	-46.86
	6	-	327.3	58.3	16.8	21.9	-	-	-	0.88	-41.78
	6.0	-	312.5	59.1	17.3	22.0	-	-	-	0.60	-47.50
	6.1	-	338.5	59.2	16.5	22.2	-	-	-	0.88	-47.52
	6.2	0.062	408.3	58.8	16.7	22.2	-	-	-	0.79	-45.67
	6.3	-	318.1	58.1	17.0	22.1	-	-	-	1.00	-46.15
	6.4	-	390.5	56.9	16.9	22.3	-	-	-	0.24	-46.38
	6.5	-	322.9	58.3	17.0	22.2	-	-	-	0.10	-47.80
	6.6	-	336.4	57.6	16.9	22.2	-	-	-	0.76	-45.54

Lake	Depth (m)	ΣH_2S (mM)	SO_4 (mM)	Cl (mM)	$\delta^{18}O_{SO4}$ (‰)	$\delta^{34}S_{SO4}$ (‰)	$\delta^{34}S_{H2S}$ (‰)	$\Delta^{34}S_{SO4-H2S}$ (‰)	$\delta^{34}S_{Elem S}$ (‰)	$\delta^{18}O_{H2O}$ (‰)	$\delta^{2}H_{H2O}$ (‰)
	6.7	-	362.2	57.9	16.8	22.2	-	-	-	-0.42	-47.87
	6.8	-	352.2	58.8	-	-	-	-	-	0.29	-47.52
	6.8	-	315.9	57.4	17.1	22.1	-	-	-	0.53	-46.68
	6.9	-	346.6	58.4	17.4	22.3	-	-	-	-	-
	6.9	-	338.3	59.0	16.8	22.1	-	-	-	0.11	-48.89
	7.0	0.19	386.4	56.9	17.9	22.5	-	-	-	-	-
	7.0	0.24	293.8	52.6	17.0	22.3	-14.8	37.1	-20.0, -20.8	-0.52	-54.84
	7.0	0.65	362.5	58.6	17.7	23.3	-14.8	38.2	-	-0.10	-47.82
	7.1	5.72	389.1	56.9	18.1	24.0	-19.0	43.0	-	-0.60	-49.36
	7.2	1.93	402.0	56.6	19.3	26.3	-24.3	50.6	-	-0.61	-50.69
	7.3	21.02	387.4	57.6	18.8	26.5	-23.1	49.5	-	-0.84	-52.76
	7.4	25.02	436.2	59.1	19.4	27.1	-23.0	50.1	-	-0.08	-51.06
	7.5	33.83	413.8	58.3	20.0	27.3	-23.7	51.1	-	-1.65	-54.55
	7.6	41.44	405.5	60.3	19.7	27.4	-24.2	51.5	-	-1.46	-57.40
	7.7	36.83	451.2	61.1	18.9	27.3	-24.0	51.4	-	-1.26	-56.4

Lake	Depth (m)	ΣH_2S (mM)	SO_4 (mM)	Cl (mM)	$\delta^{18}O_{SO4}$ (‰)	$\delta^{34}S_{SO4}$ (‰)	$\delta^{34}S_{H2S}$ (‰)	$\Delta^{34}S_{SO4-H2S}$ (‰)	$\delta^{34}S_{Elem S}$ (‰)	$\delta^{18}O_{H2O}$ (‰)	$\delta^{2}H_{H2O}$ (‰)
	7.8	39.85	436.4	60.9	18.8	27.6	-23.9	51.5	-	-1.25	-56.97
	8	34.51	522.2	61.6	19.5	27.4	-23.5	50.9	-	-1.13	-59.63
	9	31.42	459.3	66.0	19.7	28.1	-23.4	51.5	-	-2.23	-54.77
	10	34.29	524.6	67.2	19.9	28.2	-23.0	51.2	-	-1.74	-55.20
	11	40.85	412.8	65.8	19.7	27.9	-23.5	51.4	-	-2.14	-59.40
	12	29.89	428.4	67.7	19.9	28.2	-22.4	50.7	-	-1.55	-60.40
ML Pond	0	-	79.9	22.3	15.1	21.9	-	-	-	3.44	-42.55
Sleeping Lake	0	-	4.0	14.8	10.9	1.6	-	-	-	-2.81	-63.86

Table 2. Concentration and isotope data for solid phase sulfur species extracted from Mahoney Lake sediment cores recovered below the chemocline (Anoxic cores) and above the interface (Oxic core).

Core	Depth (cm)	AVS-S (wt. %)	Pyrite-S (wt. %)	Fe_{HCl} (ppm)	DOS	$\delta^{34}S_{AVS}$ (‰)	$\delta^{34}S_{Pyrite}$ (‰)	$\delta^{34}S_{organic}$ (‰)	$\Delta^{34}S_{SO4\text{-}AVS}$* (‰)	$\Delta^{34}S_{SO4\text{-}Pyrite}$* (‰)
Anoxic cores										
Core 2	1	0.33	0.25	967.1	0.89	-24.9	-24.5	-	52.6	52.2
	3	0.26	0.18	1357.4	0.82	-	-	-19.3	-	-
	4.5	0.26	0.46	1571.9	0.84	-	-	-20.9	-	-
	5.5	0.16	0.73	2376.4	0.80	-	-	-	-	-
	6.5	0.21	0.65	1750.9	0.84	-	-	-	-	-
	7.5	0.19	0.60	1510.1	0.85	-	-	-	-	-
	8.5	0.18	0.56	1409.4	0.85	-	-	-	-	-
	9.5	0.26	0.65	1548.7	0.87	-	-	-	-	-
	10.5	0.33	0.48	1196.3	0.89	-	-	-	-	-
	11.5	0.30	0.56	1282.0	0.89	-	-	-	-	-
	12.5	0.23	0.45	1417.5	0.85	-	-	-	-	-
	13.5	0.30	0.40	1068.2	0.89	-	-	-	-	-
	14.5	0.07	0.52	1716.5	0.77	-	-	-	-	-
	15.5	0.33	0.24	1437.5	0.85	-	-	-	-	-
	16.5	0.32	0.38	-	-	-	-	-	-	-
	17.5	0.26	0.22	1700.1	0.79	-26.4	-22.7	-	54.1	50.3
	18.5	0.29	0.23	1782.9	0.80	-26.8	-23.1	-	54.5	50.7
	19.5	0.35	0.22	1303.7	0.86	-26.7	-23.9	-	54.4	51.5
	20.5	0.27	0.19	1660.0	0.80	-26.4	-	-	54.1	-
	21.5	0.31	0.13	1489.0	0.82	-26.6	-22.6	-	54.2	50.2
	22.5	0.35	0.22	2230.8	0.78	-28.7	-23.1	-	56.4	50.8
	23.5	0.27	0.19	2076.9	0.76	-26.7	-22.9	-	54.3	50.6
	24.5	0.23	0.18	2227.8	0.72	-29.3	-21.2	-	56.9	48.9
	25.5	0.25	0.11	2472.4	0.69	-28.0	-22.6	-	55.7	50.2
Core 3	1	0.24	0.09	1462.4	0.78	-25.3	-19.2	-18.7	53.0	46.9
	3	0.29	0.08	1338.7	0.81	-24.4	-20.8	-19.3	52.1	48.4
	5	0.22	0.10	1350.4	0.78	-24.8	-20.6	-	52.4	48.3

Core	Depth (cm)	AVS-S (wt. %)	Pyrite-S (wt. %)	Fe_{HCl} (ppm)	DOS	$\delta^{34}S_{AVS}$ (‰)	$\delta^{34}S_{Pyrite}$ (‰)	$\delta^{34}S_{organic}$ (‰)	$\Delta^{34}S_{SO4\text{-}AVS}$* (‰)	$\Delta^{34}S_{SO4\text{-}Pyrite}$* (‰)
	7	0.18	0.13	779.5	0.85	-26.2	-21.2	-	53.9	48.9
	9	0.20	0.10	1236.8	0.78	-27.3	-21.7	-	55.0	49.3
Oxic core										
Core 9	1	0.06	0.04	910.8	0.62	-26.3	-	-16.5	48.8	-
	3	0.08	0.05	1086.3	0.62	-29.6	-	-16.9	52.1	-
	5	0.19	0.06	3085.7	0.56	-29.6	-	-	52.1	-
	7	0.15	0.06	3427.0	0.48	-29.5	-	-	52.0	-
	9	0.08	0.06	4878.7	0.28	-30.4	-	-	52.9	-
	11	0.06	0.03	1205.7	0.52	-31.4	-	-	54.0	-
	13	0.10	-	635.5	-	-32.0	-	-	54.5	-
	15	0.03	0.02	504.5	0.59	-33.3	-	-	55.8	-
	17	0.05	0.02	224.7	0.81	-33.5	-	-	56.0	-
	19	0.07	0.03	398.5	0.78	-32.5	-	-	55.0	-
	21	0.10	0.04	376.6	0.85	-32.0	-	-	54.5	-
	23	0.18	0.04	329.7	0.91	-34.8	-	-	57.3	-
	25	0.11	0.03	289.3	0.89	-33.6	-	-	56.1	-
	27	0.26	0.05	1070.0	0.82	-33.7	-	-	56.2	-
	29	0.25	0.05	682.0	0.88	-34.8	-	-	57.3	-

*$\Delta^{34}S_{SO4\text{-}sulfide}$ (where sulfide is either AVS or Pyrite) for Cores 2 and 3 are referenced to the average $\delta^{34}S$ of pore water sulfate below the chemocline ($\Delta^{34}S$ = 27.6‰ - $\delta^{34}S_{sulfide}$) and the isotopic offset for Core 9 is relative to pore water sulfate above the chemocline ($\Delta^{34}S$ = 22.5‰ - $\delta^{34}S_{sulfide}$).

Table 3. Concentration and isotope data for pore waters extracted from Mahoney Lake sediment cores recovered below the chemocline (Anoxic cores) and above the interface (Oxic core).

Core	Depth (cm)	SO_4 (mM)	Cl (mM)	ΣH_2S (mM)	$\delta^{18}O_{SO4}$ (‰)	$\delta^{34}S_{SO4}$ (‰)	$\delta^{34}S_{H2S}$ (‰)	$\Delta^{34}S_{SO4\text{-}H2S}$ (‰)
Anoxic cores								
Core 2	3	409.8	63.9	11.68	18.1	27.4	-18.7	46.2
	5.5	505.3	67.2	12.51	19.3	26.6	-21.5	48.1
	6.5	418.5	64.0	20.68	18.8	27.4	-22.4	49.7
	7.5	427.5	66.5	20.29	19.2	27.2	-23.6	50.8
	9.5	428.0	66.4	17.40	-	28.5	-20.5	-
	15.5	447.4	69.3	4.67	-	28.4	-	-
	19.5	-	-	6.05	-	-	-	-
	26.5	-	-	0.56	-	-	-	-
Core 3	0.5	468.0	69.4	18.03	19.9	28.2	-21.0	49.2
	1.5	454.0	69.7	21.36	-	-	-	-
	2.5	431.4	71.7	17.71	-	-	-	-
	5.5	453.5	70.0	15.44	-	-	-	-
	6.5	422.3	69.8	28.15	20.4	27.9	-22.6	50.5
	7.5	445.8	69.4	3.80	19.6	28.1	-20.6	48.6
	8.5	-	-	-	18.4	27.6	-25.1	52.7
	9.5	457.5	69.2	21.38	21.3	28.5	-25.0	53.5
	15	466.7	66.9	7.03	-	-	-	-
	21	473.0	69.8	15.83	-	-	-	-
	41	459.1	64.2	15.48	-	-	-	-
	53	481.7	66.7	15.80	-	-	-	-
	59	430.6	68.1	18.66	-	-	-	-
	73	440.5	68.2	8.41	-	-	-	-
	83	510.7	68.2	20.86	-	-	-	-
Oxic core								
Core 9	1	321.1	55.5	1.44	17.8	22.2	-17.8	40.1
	3	301.5	50.9	1.85	-	22.6	-30.0	52.7
	5	300.6	48.7	2.14	17.3	22.6	-24.6	47.3
	7	305.5	49.5	0.62	-	23.1	-28.3	51.5
	9	292.8	47.3	1.95	17.5	22.4	-25.4	47.8
	11	306.5	46.7	1.93	-	22.5	-25.2	47.7
	13	300.3	50.3	1.31	17.6	22.5	-27.0	49.5
	15	299.9	51.1	1.87	-	22.6	-29.9	52.5
	17	296.3	52.3	1.85	17.9	22.5	-28.7	51.2
	19	297.1	50.5	1.80	-	22.6	-29.0	51.6
	21	296.3	53.0	1.75	17.4	22.4	-36.0	58.4
	23	303.4	52.2	1.70	-	22.4	-33.6	55.9
	25	295.0	52.6	1.38	17.7	22.7	-34.5	57.2
	27	293.5	52.6	1.90	-	22.5	-	-
	29	290.3	57.3	1.38	-	22.3	-30.2	52.5